Chapter 5

The *Drosophila* 26S proteasome interactome is modulated under stress conditions as revealed by LFQ mass spectrometry.

Karen A. Sap, Dick H.W. Dekkers and Jeroen A.A. Demmers

Manuscript in preparation

Abstract

Selective proteasome-dependent degradation of proteins is important to maintain cellular homeostasis and viability under both stress and non-stress conditions. Despite extensive research, the molecular mechanism by which ubiquitin-dependent proteasomal degradation is adapted to different intracellular environments is poorly understood. Here we set out to identify differential interactor dynamics of the 19S proteasome to investigate the adaptive recruitment of specific interactors under both stress and non-stress conditions in the ubiquitin-dependent protein degradation pathway. Proteasomes were immunopurified using antibodies directed against both Rpn8 and Rpn10 from *Drosophila melanogaster* S2 cell lysates. Using a label free quantification mass spectrometry approach, we identified specific interacting proteins of the 19S/26S proteasome under various stress conditions, *i.e.* proteasome inhibition (MG132/Lactacystin), endoplasmatic reticulum stress (Tunicamycin) and oxidative stress (hydrogen peroxide). We observed an increased association of 20S core particles and 19S caps upon MG132/Lact treatment, and additionally an enhanced recruitment of several interactors including hsp23 and hsp68, REG (PA28) and ref(2)p, and a putative novel UBL-domain containing ubiquitin shuttle protein, CG7546 (Human Bat3). On the other hand, ubiquitin shuttle protein Rad23 was only found in association with the 19S cap in non-stress conditions. One other interesting finding of our study is that deubiquitinating enzyme UCHL5 was more abundant at proteasomes under all applied stress conditions, while it was clearly less recruited under non-stress conditions. Together, these data give more insight in the dynamic adaptation of ubiquitin-dependent proteasomal protein degradation under different intracellular environments. This information is relevant to understand proteasome regulation in disease states and may lead to novel therapeutic targets for the treatment of diseases in which cellular stress and homeostasis misbalance play a role.

Introduction

The 26S proteasome complex

The 26S proteasome is a 2.5-MDa enzyme complex which is responsible for the regulated degradation of a large complement of proteins in the cell (Voges, Zwickl and Baumeister, 1999; Pickart and Cohen, 2004; Finley, 2009). The 26S proteasome comprises a barrel-shaped 20S core particle (CP) and a 19S regulatory particle (RP, also known as PA700) on one or both sides (Murata et al. 2009; Ho Min Kim, Yadong Yu 2008). The 20S core subunit contains two inner heteroheptameric rings composed of Prosbeta1-7 subunits. Prosbeta1, 2 and 5 are responsible for the catalytic cleavage of proteasome substrate and exhibit respectively caspase-like, trypsin-like and chymotrypsin-like activity (Marques et al. 2009; Loidl et al. 1999). The barrel furthermore contains two outer heteroheptameric alpha rings which consist of Prosalpha1-7 subunits. These

rings function as a gate to regulate substrate entry towards the proteolytic chamber. These rings also function as docking stations for substrates, proteasome interacting proteins as well as proteasome activators, such as the 19S RP (Pickart & Cohen 2004; Groll et al. 1997).

The 19S RP regulates the proteasome-dependent degradation of polyubiquitinated substrates. This involves binding, deubiquitination and unfolding of substrate followed by opening of the 20S CP and translocation of the unfolded substrate into the catalytic core (Pickart & Cohen 2004; Verma et al. 2004; Elsasser & Finley 2005; Verma et al. 2002). The 19S RP is composed of two subcomplexes: the base and the lid (Glickman et al. 1998; Schmidt et al. 2005). The 19S RP binds with its base to the 20S CP alpha ring. The 19S base consists of a heterohexameric ring of AAA-ATPase subunits Rpt1-6 which use ATP to unfold proteasome substrate and possibly induce conformational changes of the proteasome complex upon substrate engagement. Other subunits of the base include Rpn1 and Rpn2 which function as protein interaction platforms, and ubiquitin receptors RPN10 and Rpn13. The 19S lid complex comprises eight non-ATPase subunits (RPN3, Rpn5-9, RPN11 and RPN12). Rpn11 is a deubiquitinating enzyme and the other components are probably (also) functionally supportive for the structure. The activities of the 19S RP and its assembly with the 20CP are strictly ATP-dependent.

Despite its physiological importance, many aspects of the proteasome's structural organization and regulatory mechanisms are not yet well defined. In addition to the constitutive proteasome subunits, there is increasing evidence that proteasomal function is affected by a wide variety of proteasome interacting proteins (PIPs). A broad class of PIPs has been identified, including ubiquitin ligases, ubiquitin receptors, deubiquitinases, proteasome activators and inhibitors, chaperones, and other types of modulators (Hanna et al. 2007; Finley 2009; Schmidt et al. 2005; Wang & Huang 2008; Kaake et al. 2011; Verma et al. 2000; Leggett et al. 2002; Wang et al. 2007; Guerrero 2005; Scanlon et al. 2009). These proteins interact with the proteasome in a dynamic manner in response to environmental changes and affect the function and structure of the proteasome complex.

Here, we present a systematic interactome profiling methodology to study the effects of different environmental conditions on the 19S proteasome interactome. We analyzed the adaptive recruitment of 19S interactors upon proteasome inhibition (MG132/Lact), ER stress (Tunicamycin), oxidative stress (30 min H_2O_2) and recovery after oxidative stress (24h H_2O_2) by immuno precipitations and label free quantification (LFQ)-based proteomics. Below, an overview of the stress conditions is given including the current knowledge of proteasome involvement herein.

Oxidative stress

Oxidative stress is caused by either the excessive production of reactive oxygen species (ROS) or their insufficient elimination by antioxidants (Schieber and Chandel, 2014; Tong et al. 2015) and has been implicated in aging and several diseases, such as cancer and neurodegenerative disorders. ROS are mainly produced in mitochondria (~80%), but also in peroxisomes and the endoplasmatic reticulum (ER) (Holmström & Finkel 2014; Brand 2010; Fransen et al. 2012). ROS can oxidize proteins which in turn may alter their function. Furthermore, chronic oxidative stress can result in protein misfolding. This buildup of oxidized proteins can be cytotoxic, hence the rescue of oxidized proteins by protein repair pathways or their destruction via cellular degradation pathways is of utmost importance for cell viability and the maintenance of homeostasis. The immunoproteasome could degrade oxidized proteins (Pickering & Davies 2012), but the major degradation machinery is the 20S proteasome core complex which recognizes exposed hydrophobic patches on oxidatively damaged proteins (extensively reviewed: (Goldberg 2003; Breusing & Grune 2008; Jung & Grune 2008; Raynes et al. 2016)). In contrast, the 26S proteasome is considered more vulnerable for oxidative stress (Reinheckel et al. 1998; Reinheckel et al. 2000) as the 19S and 20S particles dissociate shortly after intensive or prolonged H_2O_2-induced oxidative stress (Wang et al. 2011; Reinheckel et al. 1998). In the recovery phase the UPS was shown to be activated again (Grune et al. 2011). We set out to identify the adaptive interactome of the 19S proteasome during mild H_2O_2-induced stress and during the recovery phase.

ER stress

The ER is the site of biosynthesis of transmembrane and secreted proteins. When proteins enter the ER co-translationally, they are subsequently folded and undergo glycosylation or lipidation. The correct folding and transport of these proteins is dependent on chaperones inside the ER and on an oxidizing environment to generate disulfide bond formation between protein chains. Protein folding, modification, and transport inside the ER are strictly regulated by the protein quality control system (Wang & Kaufman 2012). ER stress emerges upon accumulation of misfolded or unfolded proteins within the ER lumen. This may be the result of various intracellular and extracellular stimuli, such as nutrient deprivation, depletion of ER calcium stores, changes in the cellular redox state, the impairment of glycosylation, impairment of vesicular transport, increased ER protein synthesis, impairment of ER-associated degradation (ERAD), or the expression of mutated ER proteins. In ER stress, unfolded proteins accumulate within the ER and this buildup affects cellular activities. Cells can respond to ER stress in two different ways, *i.e.* through survival or apoptosis. Cells can then activate the unfolded protein response (UPR) in order to survive. This response involves three different stages: 1) increasing the ER volume and decreasing protein synthesis rates (Harding et al. 1999), 2) induction of transcription of genes encoding for proteins with a role in ER protein folding and degradation (MJ Gething & Sambrook 1992), 3) induction of ERAD in order to retrotranslocate misfolded proteins from the ER to the cytoplasm for proteasome-dependent degradation (Mori 2000). By

these mechanisms, the folding capacity of the ER can be restored. We characterized the adaptive interactome of the 19S proteasome upon Tunicamycin-induced ER stress.

Proteasome inhibition mediated stress

Misregulation of the ubiquitin-proteasome system (UPS) has been associated with a number of diseases, including cancer and neurodegenerative disorders. Inhibition of the proteasome by drugs has been shown to be effective in the treatment of several types of cancers, such as the inhibitor Bortezomib for the treatment of multiple myeloma (MM). Treatment of MM cells with proteasome inhibitors (PIs) result in the accumulation of misfolded immunoglobin in the ER (Obeng et al. 2006) and hence induces the UPR (Obeng et al. 2006; Lee et al. 2003). Usually, the UPR allows the cell to survive temporary stress conditions. However, during prolonged stress conditions caused by PIs, UPR induction may lead to a cell cycle arrest (Brewer et al. 1999) and eventually the activation of apoptosis (Ri, 2016). Induction of the UPR and apoptosis by PIs is especially observed in cells with high Ig production (Meister et al. 2007). Thus, partial inhibition of proteasomes *in vivo*, which is not toxic to normal cells, may be sufficient to eliminate MM plasma cells (Meister et al. 2007). We identified the dynamic 19S interactome upon prolonged MG132/Lactacystin-induced proteasome inhibition.

Identification of proteasome interacting factors under specific stress conditions could reveal how the 26S proteasome is regulated in response to perturbations of the intracellular environment. In this study we used a label free quantitative mass spectrometry-based approach to identify the interactome of the 19S regulatory particle under different stress conditions, *i.e.* proteasome inhibition, ER-stress and oxidative stress. It is important to note that we directly target 19S subunits (Rpn8 and Rpn10) and not 20S subunits. We therefore only focus on 19S interactors as well as 26S proteasome interactors which are involved in ubiquitin-dependent protein degradation, and we do not analyze changes in alternative proteasomes. First of all we identified all constitutive 26S proteasome subunits as specific interactors in all immunoprecipitations (IP's), which validates our approach. Furthermore, we found that ubiquitin shuttle protein Rad23 was only associated with the proteasome in non-stress conditions. Additionally, we found an enhanced recruitment of deubiquitinating enzyme UCHL5 under stress conditions, to levels almost similar as general 19S subunits. A relatively unknown UBL-domain containing protein, CG7546, was identified as interaction partner of the proteasome only with proteasome inhibition. Lastly, we used relatively mild conditions for oxidative stress and we did not observe enhanced dissociation of 26S proteasomes directly after H_2O_2 treatment but on the other hand we did observe enhanced stability of the 26S proteasome upon chemical proteasome inhibition, two phenomena often described in literature (Wang et al. 2011; Reinheckel et al. 1998; Kleijnen et al. 2007). Taken together, our data gives more insight in the responses of the ubiquitin-proteasome system on stress conditions.

Results

H_2O_2 and TM induce different stress responsive genes in *Drosophila* S2 cells

We are interested in the effect of cellular stress on the composition and stability of the 26S proteasome interactome. In order to induce different types of intracellular stress, the proteasome inhibitors MG132/Lact, ER stress inducer Tunicamycin (TM) and oxidative stress inducer H_2O_2 were used for cellular perturbations. It has been shown that the 26S proteasome complex is relatively sensitive for H_2O_2 treatment (Reinheckel et al. 1998; Reinheckel et al. 2000), and that the 26S proteasome plays an important role in the recovery after oxidative stress (Grune et al. 2011). Thus, in order to maintain proper 26S proteasome homeostasis during our study we applied relatively mild oxidative stress conditions (1mM H_2O_2). First, we set out to verify the effect of H_2O_2 in *Drosophila* S2 cells by monitoring RNA expression levels of known responsive genes by Real-Time Quantitative Reverse Transcription PCR at different time points after the induction of oxidative stress (*Chow et al. 2013*). Cells were treated with 1 mM H_2O_2, which was quenched by the addition with catalase after 30 min. Total RNA was isolated from either untreated cells (0 min) or treated cells after 30 min, 1h, 4h, 8h, 16h or 24h following H_2O_2 treatment. H_2O_2 responsive genes GstD5, Hsp70 and Hsp68 were strongly upregulated already 30 min after induction and expression levels started to decline 8h after the treatment and then became relatively stable (Figure 1A). One early (30 min) and one late (24h) time point after H_2O_2 treatment were chosen for further analysis, *i.e.* the investigation of the effect of stress inducers on proteasome stability and the identification of proteasome interaction partners. Furthermore, cells were treated with 1 μM tunicamycin and total RNA was isolated at the same time points as were used for H_2O_2 treatment (Figure 1B). Tunicamycin responsive genes were selected based on results of a published quantitative mass spectrometry-based global proteome study on tunicamycin-treated human neuroblastoma cells (Bull & Thiede 2012). Induction of TM responsive genes was observed 4h after the treatment and this upregulation remained relatively stable upon prolonged exposure (Figure 1B). We used 24h treatments of 1 μM Tunicamycin in further analyses. Lastly, cells were treated with a combination of proteasome inhibitors MG132 and Lactacystin for 16h. In Chapter 3 of this thesis we have shown that 16h MG132/Lactacystin treatment causes a remarkable accumulation of ubiquitinated proteins, without severely affecting cell viability (Sap et al. 2017).

Investigation of 20S proteasome stability upon H_2O_2, TM or MG132/Lact treatment

The integrity of the proteasome complex upon MG132/Lact, TM and H_2O_2 treatment was assessed by glycerol gradient analysis (Figure 2). The largest effects were observed upon treatment with MG132/Lact. Immunoblotting glycerol gradient fractions against Prosalpha subunits revealed that MG132/Lact resulted in both an increase in lower molecular weight (sub)complexes (fractions #1-4) and higher molecular weight complexes (fractions #9-11).

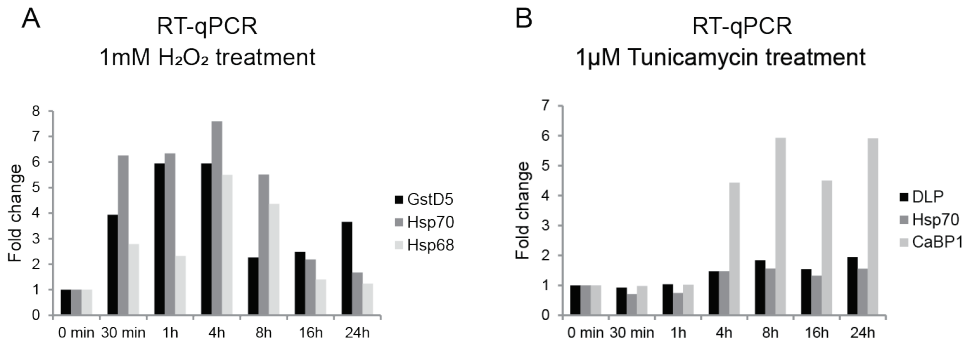

Figure 1. Upregulation of H_2O_2 and TM responsive genes. Total RNA was isolated followed by cDNA synthesis and real time RT-qPCR. Values obtained from amplification of alpha-mannosidase-lb (CG11874) were used to normalize the data as described previously (Sap et al. 2015). Fold change compared to untreated cells (0 min) is shown on the y-axis. A) Fold change upregulation of a selection of H_2O_2 responsive genes. Based on these data, treatment of 30 min and 24h were chosen as short incubation resp. long incubation time for further investigation. B) Fold change upregulation of a selection of TM responsive genes. Based on these data, treatment of 24h was chosen for further investigation.

Lower molecular weight complexes may either indicate that the proteasome became unstable or that proteasome assembly was affected, whereas the higher molecular weight complexes may suggest either the recruitment of additional proteins or protein complexes, or the formation of protein aggregates. No apparent distortion of the proteasome core complex integrity was observed upon treatment with H_2O_2 (30 min) or TM, although upon longer exposure to H_2O_2 (24 h) the appearance of higher molecular weight complexes was observed (Figure 2).

Label Free Quantification of co-immunopurified proteins of the 19S/26S proteasome
We set out to identify proteins that were recruited by the 19S/26S proteasome upon exposure to a variety of cellular stress factors. Cellular stress was induced by treatment with the following compounds: MG132 (50 µM, 16 h) and Lactacystin (5µM, 16h) ('MG132/Lact'), TM (1µM, 24 h) or H_2O_2 (1mM, 30 min or 24 h) in *Drosophila* S2 cells. Antibodies directed against the proteasome subunits Rpn8 or Rpn10 were used for immune purification (IP) of the proteasome in lysates of cells treated with the above-mentioned stress inducers and compared against untreated cells. Additional controls involve IPs with nonspecific antibodies, *i.e.* antibodies derived from rabbit preimmune serum (here referred to as 'PPI') performed in untreated cell lysates. Purified proteins were resolved by SDS-PAGE (Figure 3A, 3B, 3C) and analyzed by mass spectrometry, while quantitative analysis was performed using label free quantification (LFQ) to discriminate putative interactors from co-purifying contaminants. All IPs were performed in triplicate for solid back-end statistical analysis. Control coimmunopurifications with α-Rpn8 or α-Rpn10 antibodies showed that the proteasome subunits could efficiently be enriched for by both antibodies (Figure 3D).

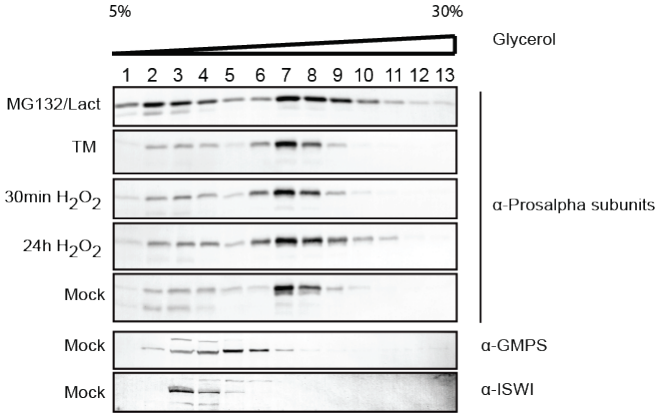

Figure 2. **TM and H_2O_2 have no major effect on proteasome stability under the tested conditions.** Cells were treated either for 16h with 50 μM MG132 and 5μM Lactacystin, for 24h with 1 μM TM, or for 30 min or 24h with 1mM H_2O_2. Mock cells were treated with DMSO only (also described as 'untreated'). Whole cell lysates were prepared under non-denaturing conditions and proteins were separated on a 5 - 30% glycerol gradient by ultracentrifugation. Proteins in the 13 different fractions were resolved by SDS-PAGE and proteasome Prosalpha subunits were visualized by immunoblotting. GMPS and ISWI were used as controls for the glycerol gradient.

To identify putative 26S proteasome interacting proteins (PIPs), proteins that were identified in the negative control (PPI) were subtracted from the data set of identified proteins in the α-Rpn8 or α-Rpn10 IPs. We used relatively stringent criteria for the selection of putative interactors, *i.e.* interactors of Rpn8 or Rpn10 should be identified in at least two replicates and statistical t-testing was used for the identification of significantly enriched proteins (Welch two-sided student T-tests, permutation-based FDR of 0.05. Number of randomizations was 250). Interactors of the 19S/26S proteasome must have been identified as specific interactors of both Rpn8 and Rpn10. In the second part of this work, where we analyze the dynamic interactome, we only take into account the proteasome interactors already identified in the first interactome study (PPI IP vs proteasome IP under both non-stress and stress conditions). With these criteria we filtered out a lot of background binders.

Figure 4 shows an overview of the proteasome interactome analysis. Proteins which were significantly enriched in either of the IPs are shown in black and known proteasome subunits are shown in red. The numbers of significantly enriched proteins in each of the IPs are listed in Table 1. We identified between 87 and 96 putative interactors of Rpn8 and between 82 and 151 putative interactors of Rpn10. The Venn diagram in Figure 5 shows the overlap of these interactors as a response to the different perturbations. Between 50 and 67 proteins were enriched in both α-Rpn8 and α-Rpn10 purifications, suggesting that these proteins are *bona fide* interactors of the 19S/26S proteasome complex.

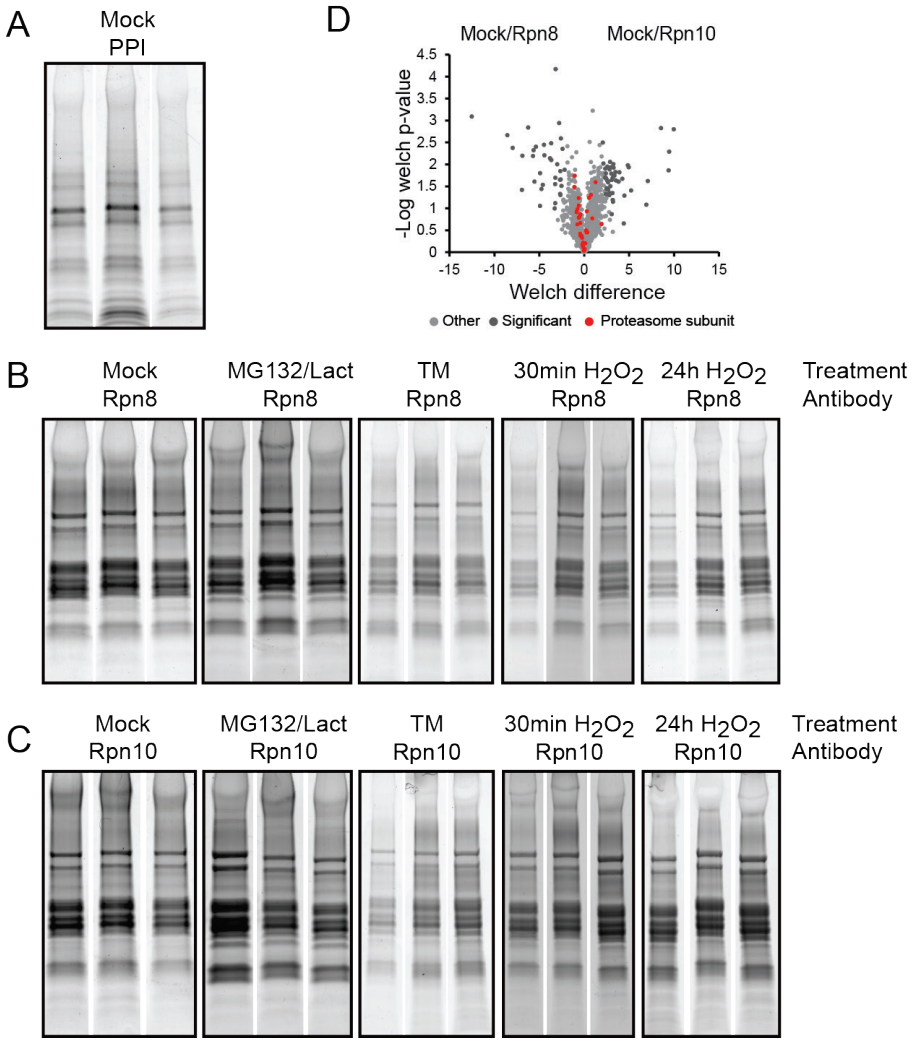

Figure 3. Immunopurification of Rpn8 and Rpn10. For each condition Immunopurification assays (IPs) were performed in triplicate from lysates of either untreated S2 cells (mock) or stress-treated cells (MG132/Lact, TM or H_2O_2). Purified proteins were resolved by SDS-PAGE and stained with Coomassie. A) IP with antibodies derived from pre-immune serum (PPI) that are not specific for proteasome subunits serve as a control for the identification of proteasome subunits and proteasome interactors. B) IPs with antibodies directed against Rpn8 under the indicated conditions. C) IPs with antibodies directed against Rpn10 under the indicated conditions. D) Welch's t-test shows that the α-Rpn8 and α-Rpn10 IPs in untreated lysates were comparable in terms of proteasome subunit (red) enrichment.

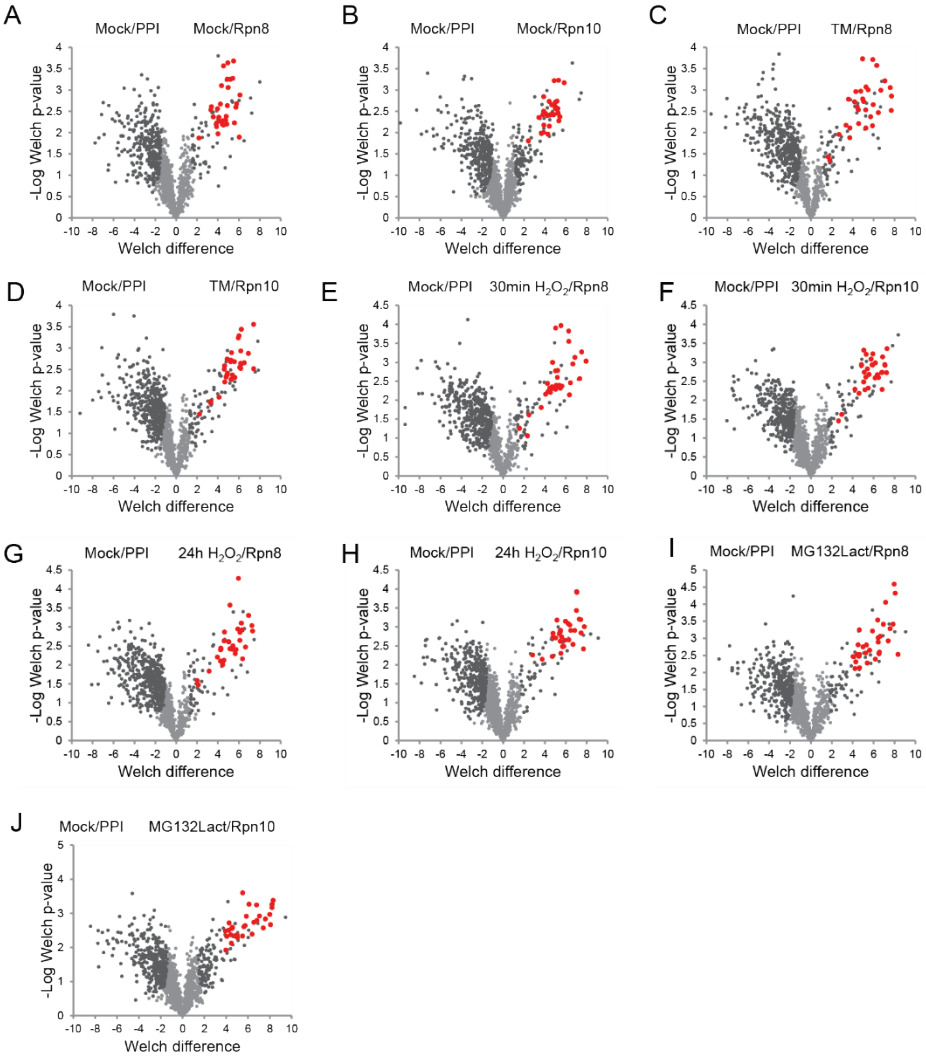

Figure 4. Identification of specific proteasome interacting proteins. Volcano plots based on Welch's t-tests performed on log2-transformed LFQ intensity values of mock treated and PPI purified samples versus A) mock-treated and Rpn8 purified samples, B) mock-treated and Rpn10 purified samples, C) TM-treated and Rpn8 purified samples, D) TM-treated and Rpn10 purified samples, E) 30min H_2O_2-treated and Rpn8 purified samples, F) 30min H_2O_2-treated and Rpn10 purified samples, G) 24h H_2O_2-treated and Rpn8 purified samples, H) 24h H_2O_2-treated and Rpn10 purified samples, I) MG132/Lact-treated and Rpn8 purified samples, J) MG132/Lact-treated and Rpn10 purified samples. Proteins enriched in the Rpn8 or Rpn10 IPs are found at the right side in each volcano plot. Proteins which were significantly enriched are shown in black; proteasome subunits are shown in red. The multi-angle comparison of Rpn8

versus mock and PPI-mock provides an extra layer of stringency, resulting in higher confidence interactor analysis.

Table 1. Numbers of significantly enriched proteins compared to PPI IP.

Immuno purification	Mock	MG132 Lact	TM	30min H_2O_2	24h H_2O_2
Rpn8 IP	87	96	87	91	89
Rpn10 IP	136	151	105	92	82
Rpn8 & Rpn10 IP	55	67	52	54	50

In general, the interactors identified with both antibodies were very similar per condition, however there were also some interesting differences. Rpn4 (CG9588/PSMD9), a chaperone involved in proteasome assembly, was enriched in all datasets, except for the α-Rpn10 IP in MG132/Lact treated cells. In addition, two E2 ubiquitin conjugating enzymes were specifically enriched in α-Rpn10 IPs in MG132/Lact treated cells: Ben/UBE2N and Effete/UBE2D2. When proteins were only enriched with the use of the Rpn10 antibody, the interaction might take place with free Rpn10 outside the proteasome. For a complete list of identified proteins for each of the purifications see Supplementary Table 1 one at the end of this chapter or online. To be sure to analyze interactors of the proteasome complex and not those for free Rpn10 we only took into account proteins that were enriched in both α-Rpn8 and α-Rpn10 IPs in all further analyses (Suppl. Table 1).

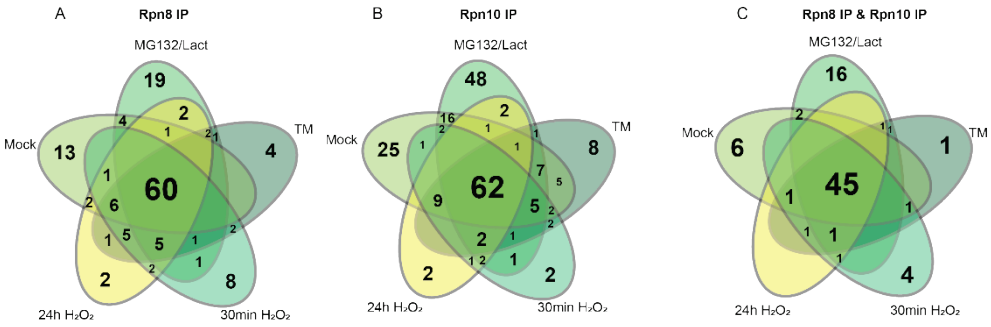

Figure 5. Overlap of significantly enriched proteins in the different IPs.
Overlap of significantly enriched proteins in A) Rpn8 purifications and B) Rpn10 purifications C) in both Rpn8 and Rpn10 purifications.

The 26S proteasome interactome independent of stress conditions

We identified 45 interaction partners of Rpn8 and Rpn10 that were present in all conditions studied here (Figure 5C). These proteins thus interacted with our bait independent of stress. Obviously, the majority of these proteins are constitutive proteasome subunits, such as the seven alpha and beta subunits of the 20S core particle. Additionally, all described 19S RP base complex constitutive subunits were identified, *i.e.* Rpt1-6 and the three non-ATPases Rpn1, Rpn2 and Rpn13, as well as all constitutive subunits of the 19S RP lid complex, Rpn3, Rpn5-9, Rpn11 and Rpn12. In conclusion, all constitutive 26S proteasome subunits were copurified through the enrichment of Rpn8 and Rpn10 in S2 cell lysates (Figure 4; Suppl. Table 1), suggesting that intact 26S proteasomes were present in all lysates. This result also validates our approach for the robust and reproducible isolation of 26S proteasomes from cell lysates.

In addition to all constitutive proteasome subunits, this data set comprises twelve additional common interactors of the 26S proteasome, some of which are known interactors that have been described in the literature. For instance, the deubiquitinating enzymes UCHL5 and USP14 were significantly enriched in all Rpn8 and Rpn10 IPs (Figure 4; Suppl. Table 1). We also identified Sem1/Rpn15, a known proteasome subunit in mammalian cells. It has been shown that Sem1 enforces incorporation of Rpn3 and Rpn7 into the assembling 26S proteasome lid complexes (Tomko & Hochstrasser 2014). However, it also functions as a stoichiometric component of the 19S RP of mature proteasomes (Bohn et al. 2013; Funakoshi 2004; Sone et al. 2004), where it has been proposed to be the third identified ubiquitin receptor of the proteasome which, unlike Rpn10 and Rpn13, interacts with ubiquitin via an unstructured ubiquitin binding site (Paraskevopoulos et al. 2014). CG12096, the *Drosophila* homolog of human S5b/PSMD5 and of yeast Hsm3, was also identified as an interaction partner in all Rpn8 and Rpn10 IPs. Hsm3 is a chaperone and supports 19S base assembly (Le Tallec et al. 2009; Barrault et al. 2012) through association with Rpt1, Rpt2 and Rpn1 (Kaneko et al. 2009). Another proteasome chaperone, CG11885, the *Drosophila* homolog of proteasome assembly chaperone 3 (PAC3), was enriched as associating factor of the proteasome in all IPs. Additionally, we identified the proteasome inhibitor Ecm29 homolog as proteasome interactor in all α-Rpn8 and α-Rpn10 IPs. Binding of Ecm29 to the proteasome induces a closed conformation of the 20S substrate entry channel and Ecm29 inhibits proteasomal ATPase activity (De La Mota-Peynado et al. 2013). Ecm29 has been proposed to couple the 26S proteasome to secretory compartments engaged in quality control and to other sites of enhanced proteolysis (endosomes, ER, ERGIC) (Gorbea et al. 2004; Gorbea et al. 2010). Ecm29 also plays a role in 26S proteasome dissociation following oxidative stress (Wang et al. 2011; Haratake et al. 2016). Furthermore, Rpt3R and Rpt6R, AAA-ATPases related to respectively Rpt3 and Rpt6, were identified as proteasome interactors in all IPs. A protein of unknown function, CG13319, was enriched in all IPs. This protein was previously found to colocalize with the proteasome in *Drosophila melanogaster* (Guruharsha et al. 2011). In addition, we identified Thioredoxin-like (Txl), the *Drosophila*

homolog of human TXNL1/TRP32, as putative interactor of Rpn8 and Rpn10. Txnl1 associates with the 19S RP directly via Rpn11 and exhibits thioredoxin activity (Andersen et al. 2009). Thioredoxins are disulfide-containing proteins that regulate the redox status of the cell and play a role in diverse oxidative cellular processes. Txl targets eEF1A1 *in vivo* (Andersen et al. 2009), which transfers misfolded nascent proteins from the ribosome to the 26S proteasome for degradation (Chuang et al. 2005). This suggests that Txl plays a role in proteasome-mediated degradation of misfolded proteins. Furthermore, ttm50 (human TIMM50/ yeast Tim50) was found to be a proteasome interactor under all conditions. Ttm50 is a member of the inner membrane translocase TIM23 complex and was picked up in a yeast two hybrid screen as an interaction partner of Prosalpha 6 (Giot et al. 2003), but a functional link between the proteasome and ttm50 has not been established yet. Finally, we identified tousled-like kinase (TLK) as a putative interaction partner of Rpn8 and Rpn10. Tlk plays a role in cell cycle progression through the regulation of chromatin dynamics (Carrera et al. 2003; Pilyugin et al. 2009). To our knowledge, the interaction of tlk with the proteasome has not been described before.

Concluding, we identified all known constitutive proteasome subunits in all purification conditions, which indicates that intact 26S proteasomes were indeed purified. Additional interactors were also identified in all purifications, some of which are well known proteasome interactors, such as UCHL5, USP14, Sem1, Ecm29 homolog and Thioredoxin-like, while several others had not been described before. These might be interesting targets for further studies.

Identification of Proteasome Interacting Proteins (PIPs) in untreated S2 cells

On top of the 45 common proteasome constituents and interaction partners identified in all IPs, 10 additional proteins were purified with both Rpn8 and Rpn10 under non-stress conditions (Suppl. Table 1). Six of these were copurified exclusively under non-stress conditions. This group comprises the phosphatase PP2A 55 kDa regulatory subunit twins (tws) Twins/tws, CG30185/Gr59f (unknown function), CG40042 (human TIMM23/yeast Tim23) (mitochondrial inner membrane translocase), Rad23, Dpck and CG13887/BCAP31.

Rad23 was copurified with Rpn10 in all conditions, although it only precipitated with both Rpn8 and Rpn10 under non-stress conditions. This suggests that Rad23 interacts with the proteasome complex only under non-stress conditions. Rad23 is known to interact with the proteasome and facilitates substrate degradation by substrate shuttling (Chen and Madura, 2002). Rad23 contains a Ubiquitin-like (UBL) domain, by which it interacts with Rpn10 (Hiyama et al. 1999; Walters et al. 2002), Rpn13 (Husnjak et al. 2008) and Rpn1 (Elsasser et al. 2002). Furthermore, it contains ubiquitin-associated (UBA) motifs that could bind specifically to K48 polyubiquitin chains and hence stimulates the interaction of K48-polyubiquitin linked substrates with the proteasome (Nathan et al. 2013). Interestingly, Rad23 is an essential component of the ERAD pathway (Medicherla et al. 2004) and functions downstream of Cdc48, which translocates misfolded or

otherwise aberrant proteins from the ER to the cytoplasm for proteasome-mediated protein degradation (Jarosch et al. 2002; Richly et al. 2005). CG13887 (human/mouse BCAP31 or BAP31), one of the most abundant ER proteins, was also identified as proteasome interactor under non-stress conditions. BCAP31 functions as a chaperone protein and targets misfolded proteins for ER-associated degradation (ERAD) (Wakana et al. 2008).

In conclusion, we identified several proteasome interactors specifically under normal, non-stress conditions, such as the proteasome substrate shuttle Rad23. Several other interacting proteins with Rpn8 or Rpn10 of diverse functions were identified.

Identification of PIPs upon proteasome inhibition by MG132/Lact

Besides the 45 common interactors described above, 22 additional proteins were copurified with Rpn8 and Rpn10 upon proteasome inhibition by MG132/Lact treatment. 16 of these interacted exclusively with the proteasome upon inhibition, including hsp23 and hsp68, REG (PA28), ref(2)p, cactus, zetaCOP, Syb, CG9306, RpS15Ab, Cisd2, DAD1, CG7375, CG12321/PAC2, CG2046 and finally CG7546 (Suppl. Table 1). Several of these proteins are known to play important roles in the UPS. For instance, CG12321 (human PSMG2/PAC2), a chaperone with a role in 20S proteasome core assembly, binds together with PSMG1 to proteasome subunits PSMA5 (*Drosophila* Prosalpha5) and PSMA7 (*Drosophila* Prosalpha4) and promotes the assembly of the proteasome alpha subunits into the heteroheptameric alpha ring and prevents alpha ring dimerization. The proteasome activator REG (REGγ/ PA28γ, human PSME3) is another interactor and is a member of the 11S/REG/PA28 family of proteins which can activate the catalytic function of the 20S proteasome (Rechsteiner & Hill 2005). The 11S proteasome activator (REG or PA28) is a heptameric structure consisting of REGα and REGβ subunits in the cytoplasm and REGγ subunits in the nucleus. These entities markedly activate the peptidase activities of the 20S proteasome but do not promote degradation of intact proteins in general (Chu-Ping, Clive A. Slaughter, et al. 1992), although it has been shown to be able to degrade several intact proteins like the steroid receptor coactivator SRC-3 (Li et al. 2006), the HCV core protein (Moriishi et al. 2007) and the cell cycle regulators p21 (Chen et al. 2007) and p53 (Zhang & Zhang 2008). Furthermore, Refractory to Sigma P (Ref(2)p), the *Drosophila melanogaster* homolog of mammalian p62, was found to associate with the proteasome exclusively upon inhibition. P62 functions as a shuttle for ubiquitinated proteins (Pankiv et al. 2007) with a preference for Lys63 ubiquitination and consequently primarily targets proteins for autophagy. However, it also interacts with Lys48 polyubiquitin chains and can thus also shuttle proteins for proteasomal degradation (Seibenhener & Babu 2004). UBL-domain containing protein CG7546 is another factor that associated exclusively with the proteasome upon MG132/Lact treatment. Homologous UBL-domains are found in the Xenopus leavis and human Scythe/Bat3 proteins, and Scythe was shown to interact with a specific splice variant of Rpn10 in Xenopus proteasomes (Kikukawa et al. 2005).

Interestingly, the heat shock proteins, Hsp23 and Hsp68 also associate with the proteasome upon proteasome inhibition. The heat shock protein family is a highly conserved protein family which accounts for 1–2% of the total protein pool. Although not all functions of HSPs are clear, most of them function as molecular chaperones to assist in folding of newly synthesized, misfolded and damaged proteins and as such are part of a major quality control system. In Chapter 3 of this thesis, we have described a major upregulation of many Hsp's upon proteasome inhibition. These results suggest that at least some of these physically interact with the proteasome either directly or via the substrate.

Other proteins that exclusively interacted with the proteasome upon MG132/Lact treatment in our screen include mitochondrial membrane protein CG1458 (human CISD2) and the 40S ribosomal protein S15Ab, which is a structural constituent of the ribosome. Also, Cactus (human NFKB1A), a protein that acts as a negative regulator of the NF-kappa-B signaling pathway was co-precipitated in Rpn8 and Rpn10 IPs upon proteasome inhibition. Additionally, CG7375 (human Ube2M/NEDD8-conjugating enzyme Ubc12), a NEDD8 conjugating enzyme which is, together with E3 ubiquitin ligase RBX1, involved in cell proliferation via neddylation of cullins, were enriched with Rpn8 and Rpn10 upon MG132/Lact treatment. Further research is required in order to address the role of many of these interactions with the proteasome.

Proteasome activator PI31 interacts specifically with the 19S/26 proteasome upon stress induction.

The proteasome activator PI31 associated with the proteasome in all applied stress conditions and in non-stress conditions it co-precipitated only with Rpn10. PI31 is the *Drosophila* homolog of human PSMF1 and was originally identified and characterized as an in vitro inhibitor of the 20S proteasome activity (Chu-Ping, Clive A Slaughter, et al. 1992; Bader et al. 2011; Mccutchen-Maloney et al. 2000). Additionally, via interaction with the 20S core particle, PI31 can inhibit the assembly of both 26S proteasomes and PA28 proteasomes by blocking interaction with 19S subunits and, respectively, 11S subunits *in vitro* (Zaiss et al. 1999; Mccutchen-Maloney et al. 2000). Interestingly, in contrast to the inhibitory effect on the 20S proteasome, PI31 has also been found to enhance the activity of 26S proteasomes both *in vitro and in vivo* (Bader et al. 2011). PI31 can act as a selective modulator of the proteasome-dependent steps in MHC class I antigen processing and can interfere with the maturation of immunoproteasome precursor complexes (Zaiss et al. 2002). More research is required in order to determine the role of PI31 at the 26S proteasome in more detail, especially in relation with cellular stress conditions.

Identification of PIPs upon ER-stress or oxidative stress

Only a subset of proteasome interacting proteins copurified specifically upon ER stress or oxidative stress, *e.g.* Tspo, a translocator protein located in the outer mitochondrial membrane. Superoxide dismutase (Sod2), an antioxidant protein which can protect the cell against excessive reactive oxygen species, was only identified under TM-induced ER stress conditions. On the

other hand, four proteins interacted specifically with Rpn8 and Rpn10 upon short oxidative stress exposure, *i.e.* AP-1sigma, ATPsynG, CG9662 and CG30159. AP-1sigma is involved in vesicle mediated transport. ATPsynG is involved in ATP synthesis coupled proton transport. CG9662 plays a role in translocating proteins across the rough ER membrane, while CG30159 is a protein with yet unknown function. Further research is required in order to address the role of these interactions with the proteasome.

Identification of dynamic proteasome interacting proteins by label free quantification
Next, we applied label free quantitative (LFQ) mass spectrometry to investigate the dynamics of the proteasome interactome by characterizing differential recruitment of interactors between mock-treated samples and stress-treated samples. Figure 6 shows an overview of the results; the numbers of proteins that were specifically enriched for are listed in Table 2, while a more detailed table can be found online (Suppl. Table 2). Here, we focused solely on proteins which were differentially recruited as a result of the perturbation, while the proteasome IP´s under non-stress conditions were treated as controls. Only proteins that were already identified as specific proteasome interactors in the previously described analysis were accepted (grey rows in Table 2).

The abundance of several proteasome subunits was clearly affected upon stress (Figure 6, Table 3). Upon MG132/Lact treatment larger amounts of 20S core proteasome subunits were copurified, which might be the result of the inhibition of 26S proteasome dissociation by the binding of the chemical proteasome inhibitors (Kleijnen et al. 2007). Several studies report dissociation of 19S and 20S subunits following oxidative stress (Wang et al. 2011; Reinheckel et al. 1998; Haratake et al. 2016). We therefore used relatively mild conditions (1mM H_2O_2) which did not lead to dissociation and is in agreement with other studies (Wang et al. 2011; Reinheckel et al. 1998). We like to mention again that Figure 1 shows that we obtained a proper stress response upon H_2O_2 treatment.

UCHL5 was identified as a specific interactor in all purifications, but by assessing the dynamic interactome we clearly see an enhanced recruitment of this enzyme under all applied stress conditions as compared to non-stress conditions. In contrast, another deubiquitinase, USP14, was associated with the proteasome to a lesser extent as a result of H_2O_2 and TM treatment. Furthermore, the 19S subunits Rpn8, Rpn9, Rpn11, Rpn12 and Rpn13 were enriched in one or two of the applied stress conditions. However, it should be noted that the variation between the different samples is relatively small. Upon MG132/Lact treatment, several more interacting proteins were increasingly enriched compared to non-stress conditions, such as proteasome assembly chaperone CG12321/PAC2, proteasome inhibitor ECM29 homolog, proteasome activator REG, Hsp70, Hsp23 and Hsp68, ref(2)P, zetaCOP (involved in endosomal trafficking) and the ER-membrane protein DAD1. Finally, several proteins became less enriched upon the imposed cellular stress, such as Apoptosis Inducing Factor (AIF), Cisd2 and tws.

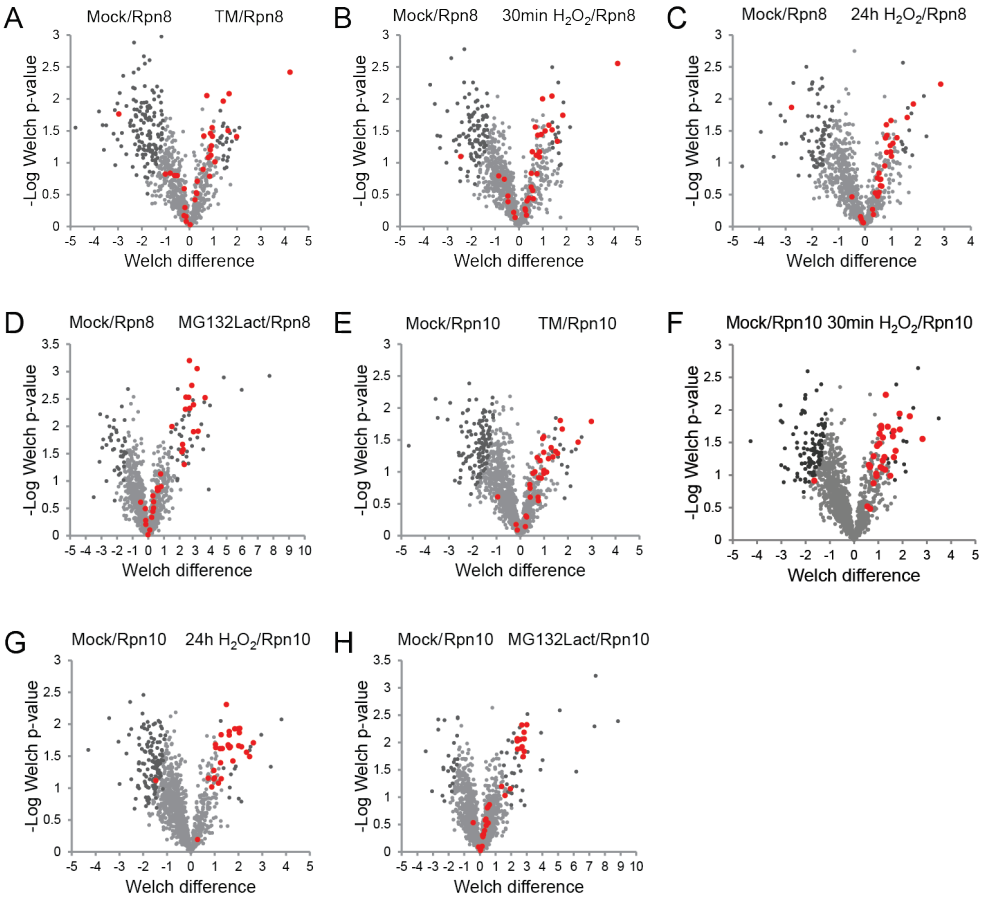

Figure 6. Identification of differential and specific interactors for each stress condition. Volcano plots based on Welch's t-tests performed on log2-transformed LFQ intensity values of proteins identified and quantified in mock-treated cells versus stress-treated cells. Rpn8 was used as the bait in panels A-D; the treatments were A) TM, B) 30 min H_2O_2, C) 24 h H_2O_2 and D) MG132/Lact. Rpn10 was used as the bait in panels E-H the treatments were E) TM, F) 30 min H_2O_2, G) 24 h H_2O_2 and H) Mg132/Lact. Proteins which were significantly more enriched are shown in black. Proteasome subunits are shown in red.

Table 2. Numbers of recruited interactors in stress conditions. Numbers of significantly enriched proteins in stress-treated lysates are shown in the table. Numbers of proteins which were significantly enriched in both Rpn8 and Rpn10 IPs and additionally were identified as specific proteasome interactors in the previously described analysis (Suppl. Table 1) are shown in the grey colored rows. These proteins were selected for further investigation.

Immuno purification	Side volcano plot	MG132/Lact	TM	30min H_2O_2	24h H_2O_2
Rpn8 IP	Left	41	139	101	76
Rpn10 IP	Left	27	121	111	133
Rpn8 & Rpn10 IP	Left	4	39	32	24
Rpn8 IP & Rpn10 IP – PPI & Mock	Left	0	2	1	1
Rpn8 IP	Right	52	30	22	15
Rpn10 IP	Right	51	25	24	35
Rpn8 IP & Rpn10 IP	Right	28	7	5	4
Rpn8 IP & Rpn10 IP – PPI & Mock	Right	28	3	4	4

UCHL5 was identified as a specific interactor in all purifications, but by assessing the dynamic interactome we clearly see an enhanced recruitment of this enzyme under all applied stress conditions as compared to non-stress conditions. In contrast, another deubiquitinase, USP14, was associated with the proteasome to a lesser extent as a result of H_2O_2 and TM treatment. Furthermore, the 19S subunits Rpn8, Rpn9, Rpn11, Rpn12 and Rpn13 were enriched in one or two of the applied stress conditions. However, it should be noted that the variation between the different samples is relatively small. Upon MG132/Lact treatment, several more interacting proteins were increasingly enriched compared to non-stress conditions, such as proteasome assembly chaperone CG12321/PAC2, proteasome inhibitor ECM29 homolog, proteasome activator REG, Hsp70, Hsp23 and Hsp68, ref(2)P, zetaCOP (involved in endosomal trafficking) and the ER-membrane protein DAD1. Finally, several proteins became less enriched upon the imposed cellular stress, such as Apoptosis Inducing Factor (AIF), Cisd2 and tws.

Table 3. Log2 transformed LFQ intensities and significantly enriched proteins ('+') in α-Rpn8 and α-Rpn10 IPs under cellular stress conditions

												More abundant on proteasome w. stress				More abundant on proteasome w/o stress			
ProtID	Protein names	Mock_Rpn8	MG132_Rpn8	TM_rpn8	H2O2 30 min_rpn8	H2O2 24h_rpn8	Mock Rpn10	MG132 Rpn10	TM Rpn10	H2O2 30 min Rpn10	H2O2 24h Rpn10	MG132/Lact	TM	30min H2O2	24h H2O2	MG132/Lact	TM	30min H2O2	24h H2O2
E1JGZ9	Prosalpha1	30	32	29	29	30	31	33	31	31	32	+							
P40301	Prosalpha2	30	32	29	29	29	30	33	31	31	32	+							
P18053	Prosalpha3	29	32	29	28	29	30	33	30	31	32	+							
P22769	Prosalpha4	29	32	29	29	30	30	33	30	32	32	+							
Q95083	Prosalpha5	29	31	28	29	28	30	32	30	31	31	+							
P12881	Prosalpha6	28	32	28	29	29	30	33	31	31	32	+							
Q9V5C6	Prosalpha7	29	31	29	28	29	30	33	31	31	32	+							
A0AQH0	Prosbeta1	29	31	29	29	29	29	32	30	31	32	+							
Q9VUJ1	Prosbeta2	29	31	29	29	29	30	32	30	31	32	+							
Q9XYN7	Prosbeta3	28	31	28	29	29	29	32	30	30	31	+							
Q9VJJ0	Prosbeta4	29	31	28	29	29	29	32	30	31	32	+							
Q7K148	Prosbeta5	29	31	28	28	28	29	32	30	30	31	+							
P40304	Prosbeta6	29	31	28	29	29	30	33	30	31	31	+							
Q9VNA5	Prosbeta7	28	31	28	28	28	29	32	30	30	31	+							
Q7KMQ0	Rpt1	33	34	34	34	34	34	34	35	35	35								
P48601	Rpt2	33	34	34	34	34	34	34	34	35	34								
Q9V405	Rpt3	34	34	35	35	34	34	35	35	35	35								
Q9W414	Rpt4	33	34	34	34	34	34	34	35	35	35								
Q9V3V6	Rpt5	33	33	34	34	34	33	34	34	34	34								
O18413	Rpt6	34	34	34	34	34	34	34	35	35	35								
Q9VW54	Rpn1	35	35	35	36	36	35	35	36	36	36								
Q9V3P6-2	Rpn2	35	36	36	36	36	35	35	36	36	37								
M9PG62	Rpn3	34	34	35	35	35	34	34	35	35	35								
Q9V3Z4	Rpn5	34	34	35	35	35	34	34	35	35	35								
Q7KLV9	Rpn6	34	34	35	35	35	34	34	35	35	35								
Q9V3G7	Rpn7	34	34	35	35	35	33	34	35	35	35								
P26270	Rpn8	33	34	35	34	35	33	34	34	35	35				+				
Q7KMP8	Rpn9	33	34	35	35	35	33	34	34	35	35				+				
M9PIG8	Rpn10	32	33	33	33	33	33	33	35	35	35								
Q9V3H2	Rpn11	33	33	35	35	34	33	33	35	34	34		+	+					
Q9V436	Rpn12	33	33	35	34	35	33	33	34	35	35			+	+				
Q7K2G1-2	Rpn13	33	34	34	34	34	33	34	34	34	35		+	+					
Q9XZ61	UCHL5	29	32	33	33	31	30	32	33	33	33	+	+	+	+				
Q9VKZ8	USP14	27	26	24	24	24	28	28	27	26	26								+
Q9V677	ECM29 homolog, CG8858	30	32	29	29	29	30	32	30	30	31	+							
P02825	Hsp70Aa	27	30	29	29	29	29	31	29	30	29	+							
M9NE68	Hsp23	24	27	22	23	23	22	28	21	22	22	+							
O97125	Hsp68	22	27	23	24	24	24	27	24	25	25	+							
Q9V3P3	REG	27	30	27	27	27	26	31	26	26	25	+							
P14199	Protein ref(2)P	22	26	20	22	21	24	28	23	24	23	+							
Q8IQP2	zetaCOP	22	24	21	22	21	24	26	23	23	23	+							
Q9VLM5	DAD1	22	26	23	23	21	25	28	25	25	24	+							
Q9VEC2	CG12321	20	27	20	20	20	22	29	22	22	24	+							
Q9VQ79	AIF	23	23	21	22	21	24	24	22	23	23						+		
Q9VAM6	Cisd2	25	26	23	24	24	26	27	25	25	26						+		
P36872	tws	26	24	22	22	23	26	25	25	24	26							+	

In conclusion, using LFQ proteomics we observed the dynamic interaction of proteasome subunits and proteasome-interacting proteins that was dependent on cellular stress. We purified more 26S proteasomes upon proteasome inhibition. Interestingly, co-purification of UCHL5 was enhanced upon stress induction, while USP14 was less efficiently enriched, suggesting distinct roles for these DUBs. Other proteins that became increasingly enriched upon MG132/Lact treatment include the proteasome inhibitor ECM29, heat shock proteins, the proteasome activator REG and Ref(2)p. Recruitment of these factors to the proteasome under stress conditions may indicate that the UPS interfaces with diverse cellular processes.

Discussion

19S/26S interactome (in)dependent of stress conditions

Using both α-Rpn8 and α-Rpn10 antibodies we have immunopurified 19S particles and intact 26S proteasomes from cell lysates to study both the interactome as well as the dynamic interactome of the 19S particle under both stress and non-stress conditions. All constitutive proteasome subunits were identified independent of the used conditions. Besides these constitutive subunits, a variety of additional interactors were identified in all purifications, including several chaperones with a role in proteasome (dis)assembly, activators and inhibitors and UCHL5, USP14, Sem1, ECM29 homolog and Thioredoxin-like. Identification of these 26S proteasome constitutive subunits and well-known interactors in all purifications validates our approach to specifically enrich 19S as well as 26S proteasomes from S2 cell lysates.

Our data give novel insights into proteasome composition dynamics upon non-stress and stress conditions. For instance, Ub shuttle protein Rad23 was identified as a proteasome interactor under non-stress conditions. But under stress conditions only the interaction with Rpn10 was maintained, while interaction with Rpn8 was lost, suggesting that Rad23 interacts with free Rpn10 outside the proteasome complex under stress conditions. This observation raises several questions. For instance, it is unclear why Rad23 is only enriched for the 26S proteasome under non-stress conditions and what the function of a Rpn10-Rad23 complex outside the 26S proteasome would be. It was shown before that free Rpn10 inhibits the interaction of Ub shuttle protein Dsk2 and the proteasome in budding yeast (Matiuhin et al. 2008). In this way free Rpn10 could be used to regulate the delivery of ubiquitinated substrates to the proteasome via shuttle protein Dsk2 (Matiuhin et al. 2008). Our data might point in a similar direction: free Rpn10 may also inhibit the interaction of Rad23 with the proteasome, but then only under stress conditions. Obviously, additional experiments are required to elucidate the mechanism behind the interplay of ubiquitin receptor Rpn10 and the shuttle factor Rad23 in both stress and non-stress conditions.

Refractory to Sigma P (Ref(2)p)/human p62 was identified as an interactor of the proteasome upon MG132/Lact mediated inhibition. We have shown before that the pharmacological inhibition of the proteasome increased Ref(2)p expression levels (Sap et al. 2017) and it is also known that Ref(2)p interacts with Rpt1 (Seibenhener & Babu 2004; Geetha et al. 2008) and that it serves as a substrate shuttling factor for proteasomal degradation (Geetha et al. 2008). Our data suggest that the interaction of Ref(2)p with the 26S proteasome is dependent on the inhibition status of the proteasome. However it should be excluded whether we identified more Ref(2)p as a result of MG132/Lact-induced increased 26S proteasome stability.

In addition, we observed specific physical interactions of stress responsive proteins (Hsp's) upon proteasome inhibition and oxidative stress. Hsp's function as chaperones that mediate proper folding of substrate proteins with non-native conformations, thereby protecting substrates from aggregation. Chaperones are also involved in proteasome-dependent degradation of misfolded proteins. Hsp70s are among the most prominent chaperone families that assist in chaperone-mediated proteasomal degradation of misfolded proteins (Kettern et al. 2010; Arndt et al. 2007). They can improve recognition of the substrate by ubiquitin ligases and shuttle them to the proteasome once they are ubiquitinated. Additionally, HSP70 is also involved in dissociation of 26S proteasome complexes into free 20S particles and bound 19S regulators and in reconstitution of 26S proteasomes shortly after mild oxidative stress (Grune et al. 2011). We immunopurified 19S particles and our data clearly shows that we enriched for 26S proteasomes but also 19S alone. It might be possible that Hsp70 which we identified in our screen is the interacting chaperone of free 19S particles. Finally, chaperones are also able to affect proteasome activity. It has been shown that HspP27 interacts directly with the 26S proteasome and with polyubiquitin, and that overexpression of Hsp27 increases the activity of the proteasome upon stress induction by inflammatory cytokines and cytotoxic drugs (Parcellier et al. 2003). Our data suggest that chaperones also play a role in proteasome-dependent degradation upon treatment with chemical proteasome inhibitors, however here as well it should be excluded whether we precipitated more heat shock proteins as a result of increased proteasome levels due to proteasome inhibition.

CG7546, a protein of yet unknown function, was found to interact with the proteasome exclusively upon cytotoxic stress induction. Its homolog in Xenopus, Scythe, interacts with a splice variant of Rpn10 (Kikukawa et al. 2005). CG7546 bears furthermore structural similarity to Bag6, who's N-terminal UBL domain suggests involvement in protein degradation (Minami et al. 2010). Bag6 is known to interact with pro-apoptotic proteins and targets them to Rpn10 for subsequent proteasome-dependent degradation (Kikukawa et al. 2005). Thus, CG7546 might be a novel shuttle factor involved in targeting substrates to the proteasome.

Proteasome activator PI31 was specifically interacting with the proteasome in all tested stress conditions, in non-stress conditions it only interacted with Rpn10. The molecular mechanism by which PI31 affects proteasome activity remains unknown. A previous study showed that PI31

can increase the activity of the 26S proteasome *in vivo* under conditions where maximal proteolytic activity is required, for instance for the removal of cellular proteins during the terminal differentiation of sperm (Bader et al. 2011). Similarly, PI31 activity might also be beneficial for boosting the degradation of rapidly and highly elevated proteasome substrate loads during cellular stresses in our experiments.

Dynamic 19S/26S interactome during stress and non-stress conditions

The abundance of several purified proteasome subunits was clearly affected upon stress (Figure 6, Table 3). More intact 26S proteasomes were enriched upon proteasome inhibition, which might be the result of decreased proteasome disassembly through the use of proteasome inhibitors (Kleijnen et al. 2007). We furthermore used relatively mild oxidative stress conditions since the 26S proteasome is relatively sensitive for this type of stress (Reinheckel et al. 1998; Reinheckel et al. 2000). Therefore, we did not observe enhanced dissociation of 19S and 20S particles following H_2O_2 treatment, which is in agreement with other studies (Reinheckel et al. 1998; Wang et al. 2011).

Interestingly, we observed an enhanced interaction of deubiquitinating enzyme UCHL5 with the proteasome under stress conditions. In general, the role of UCHL5 at the proteasome has not been clearly defined yet and could be multifaceted and for now we could only speculate about the role of UCHL5 at the proteasome during stress. It has for instance been proposed that UCHL5 performs an editing function by removing distal ubiquitin moieties from polyubiquitin chains and that this might be a method by which inadequately targeted proteins can be released from the proteasome and spared from degradation (Lam et al. 1997). Since UCHL5 is recruited and activated by Rpn13, the editing function of UCHL5 might be specific for Rpn13 targeted substrates, which might be important during stress conditions. Alternatively, UCHL5 could play a role in the deubiquitination of proteasome subunits. At least four proteasome subunits are targets for regulatory ubiquitination: Rpn10, Rpn13, UCHL5 and Rpt5 (Jacobson et al. 2014). Ubiquitination of these proteasome subunits impairs substrate binding, deubiquitination and degradation. The ubiquitination of these proteasome subunits is also influenced by certain cellular stress (Jacobson et al. 2014). For instance, the ubiquitination of all four proteasome subunits was found to be decreased upon H_2O_2 and MG132 treatment (Jacobson et al. 2014). Our results may indicate that decreased proteasome ubiquitination under stress conditions could be the result of increased UCHL5 recruitment and, thus, an increased deubiquitinating activity. Another possibility is that UCHL5 breaks down unanchored polyubiquitin chains that bind to proteasome-associated ubiquitin receptors and thereby block substrate access (Zhang et al. 2011). This process could be useful under stress conditions, when the proteasome substrate load is increased. It should be noted that UCHL5 is also present outside the proteasome, albeit in a non-active form as part of the chromatin remodeling INO80 complex (Yao et al. 2008), but we did not pick up any of the INO80 complex subunits as interactors in our screen.

Upon MG132/Lact treatment, several interacting proteins were increasingly enriched compared to non-stress conditions, such as proteasome assembly chaperone CG12321/PAC2, proteasome inhibitor ECM29 homolog, proteasome activator REG, Hsp70, Hsp23 and Hsp68, ref(2)P, zetaCOP (involved in endosomal trafficking) and the ER-membrane protein DAD1. We however also found an enrichment of intact 26S proteasomes upon MG132/Lact treatment. Therefore, it should be determined whether enhanced enrichment of interacting partners was due to enhanced recruitment or due to enhanced 26S proteasome levels.

Concluding remarks

Although we did several interesting findings as described above, in general we did not observe many specific effects for each individual stress that we applied. This might be explained in several ways. First, there is a lot of cross talk between the induced regulatory pathways and cellular responses inflicted by the different stress conditions. For instance, proteasome inhibition (Obeng et al. 2006; Lee et al. 2003), ER stress (Oslowski & Urano 2013) and oxidative stress (Kupsco & Schlenk 2015) may all induce the unfolded protein response (UPR). Furthermore, proteasome inhibition may lead to ER stress due a diminished removal of damaged and misfolded proteins (Bush et al. 1997). Additionally, proteasome inhibition may induce oxidative stress (Fribley et al. 2004), but an opposite effect is also observed in some cell types (Yamamoto et al. 2007). Cross-talk between the different stress conditions makes it difficult to distinguish specific responses for each individual condition. Second, in this study we used LFQ-based quantitative proteomics in combination with immune purifications (IPs) to study the differential recruitment of proteasome interactors. IPs are primarily suitable to identify stable interactors. Techniques which might be applied in order to pick up more transient interactors are BioID (Varnaite & MacNeill 2016) and APEX (Kim & Roux 2016), this might however give more background/false positive hits. Thirdly, in this study we focused on enrichment of 19S caps, however, changes might also be found in other proteasome caps, such as PA28αβ, PA28γ, PA200, PI31, or in solely the standard 20S proteasome or the immunoproteasome. These different proteasome complexes could be separated from each other by fractionation on glycerol gradients followed by LC-MS/MS and protein correlation profiling (Fabre et al. 2015). Fourth, proteasome activity may also be regulated at the level of post translational modifications (PTMs). For instance, it has been demonstrated that ubiquitination of Rpn10, Rpn13, UCHL5 and Rpt5 impairs substrate binding, deubiquitination and degradation (Jacobson et al. 2014). In fact, more than 345 sites at the proteasome can be modified and 11 different modifications were identified, reviewed in (Hirano et al. 2015). Thus, differential modification of proteasome subunits with and without stress might also contribute to altered proteasome regulation.

Finally, our data show that the combination of classical immune purifications with LFQ-based quantitative proteomics is a powerful approach to specifically detect (sub)stoichiometric interaction partners, as well as dynamic interactors, of a large and important cellular machinery. We identified several proteasome interactors, which responded differently upon stress

conditions, such as UCHL5, Rad23, CG7546 and Ref(2)p. Further research is required to elucidate their function in proteasome-dependent degradation in conditions with and without stress. Differential proteasome interactors upon specific stressors may act as therapeutic targets for the treatment of diseases in which cellular stress and homeostasis misbalance play a role.

Material and Methods

Cell culture. *Drosophila melanogaster* Schneider's line 2 cells (S2 cells) (R690-07, Invitrogen) were cultured in Schneider's medium (Invitrogen) supplemented with 10% fetal calf serum (Thermo) and 1% Penicillin-Streptomycin. Cells were treated for 16h with 50 μM MG132 and 5μM Lactacystin (MG132/Lact), or for 24h with 1μM TM (Sigma), or for 30 min or 24h with 1mM H_2O_2 (Invitrogen). For H_2O_2 treatments, cells were incubated in serum free medium and directly exposed to H_2O_2. After 30 min H_2O_2 was quenched with catalase and two volumes of complete medium was added. Cells were harvested directly (30 min) or after 24h.

Antibodies. Polyclonal antibodies were generated by immunizing rabbits with GST fusion proteins expressed in *Escherichia coli* and were affinity purified as described previously (Chalkley & Verrijzer 2004). The full length Rpn8 and full length Rpn10 were used as antigens. Pre-immune serum (PPI) of Rpn10 immunized rabbit was used. SDS-PAGE and Immunoblotting experiments were performed as described previously (Chalkley et al. 2008).

RNA isolation and real time RT-qPCR. For gene expression assays, cell pellets were immediately frozen in liquid nitrogen and -80°C until further processing. Total RNA was extracted from 5x10^6 cells using Trizol (15596-026, Invitrogen) and 4 μg RNA was used for random hexamer primed cDNA synthesis using the Superscript II Reverse Transcriptase (Invitrogen). Quantitative real-time RT-PCR was performed on a CFX96 realtime PCR detection system (Bio-Rad). Reactions were performed in a total volume of 25 μl containing 1x reaction buffer, SYBR Green I (Sigma), 200 μM dNTPs, 1.5 mM MgCl2, platinum Taq polymerase (Invitrogen), 500 nM of corresponding primers and 1 μl of cDNA. The primer sequences used were GstD5: 5'-TATGCCAACGCCAAGAAGGT-3', 5'-CGGCACCTTTCCAGTTCTCT-3'; Hsp70: 5'-AAGAACCTCAAGGGTGAGCG-3', 5'-CGTCGATGGTCAGGATGGAG-3'; Hsp68: 5'-AGCAACAGAAATAGCCAAGATGC-3', 5'-GTGTGGTACGGTTACCCTGG-3'; DLP: 5'-CTAGCAGCTCGGGATCACTG-3', 5'-TCGCTCTCGGCTTTTGTGAA-3'; CaBP1: 5'-TGTTGCTGGCATTTGTCGTG-3', 5'-ATCGCTGGGCGAATAGAAGG-3'. Data analysis was performed by applying the 2-ΔΔCT method (Livak & Schmittgen 2001). Values obtained from amplification of α-Mannosidase class I b (CG11874) were used to normalize the data as described previously (Moshkin et al. 2007).

Glycerol gradient. Preparation of glycerol gradients is previously described (Mohrmann et al. 2004). Briefly, gradients with 5% - 30% glycerol were made in Beckman polyallomer tubes (331374 Beckman). Whole cell lysates were made under non-denaturating conditions (50 mM HEPES-KOH pH 7.6, 100 mM KCl, 0.1% NP40, protease inhibitors), loaded on top of the gradient and ultracentrifuged (SW40 rotor, Beckman L-80) with 32 krpm for 17h by 4°C. Approximately 26 x 500 µl fractions were taken starting from the top of the gradient with a P1000 pipet. Fractions were stored in aliquots in -80°C. Two consecutive fractions were combined starting from fraction 3, which resulted in a total of 13 fractions. Of each fraction, 25 µl was resolved by SDS-PAGE and visualized by immunoblotting.

Immuno purifications. Immunopurification (IP) procedures were performed essentially as described (Chalkley & Verrijzer 2004). Briefly, α-Rpn8 or α-Rpn10 antibody was crosslinked to ProtA beads (GE Healthcare) by using dimethylpimelimidate. As a control, antibodies from pre-immune serum were coupled to ProtA beads. After 2 h incubation of the antibody coupled beads with whole cell lysate (125x10^6 cells), the beads were washed extensively with HEMG-based washing buffer (25mM HEPES-KOH, pH 7.6, 0.1mM EDTA, 12.5mM MgCl2, 10% glycerol, 200mM KCl, 0.1% NP-40, containing a cocktail of protease inhibitors). Proteins retained on the beads were eluted with 100mM sodium citrate buffer (pH 2.5), TCA precipitated, resolved by SDS-PAGE and visualized by Coomassie staining. Lanes were cut in 1 mm slices and combined to in total 13 fractions per lane and analyzed by LC-MS/MS.

Mass spectrometry. In-gel protein reduction, alkylation and tryptic digestion was done as described previously (van den Berg et al. 2010). Peptides were extracted with 30% acetonitrile 0.5% formic acid and analyzed on an 1100 series capillary LC system (Agilent Technologies) coupled to an LTQ-Orbitrap hybrid mass spectrometer (Thermo). Peptide mixtures were trapped on a ReproSil C18 reversed phase column (Dr Maisch GmbH; column dimensions 2 cm × 100 µm, packed in-house) at a flow rate of 8 µl/min. Peptide separation was performed on a ReproSil C18 reversed phase column (Dr Maisch GmbH; column dimensions 15 cm × 75 µm, packed in-house) using a linear gradient from 0 to 50% B (A = 0.1% formic acid; B = 80% (v/v) acetonitrile, 0.1% formic acid) in 120 min at a constant flow rate of 300 nl/min (using a splitter for the 1100 system). The column eluent was directly electrosprayed into the mass spectrometer. Mass spectra were acquired in continuum mode; fragmentation of the peptides was performed in data dependent acquisition mode by CID using top 8 selection.

LFQ data analysis. RAW files were analyzed using MaxQuant software (v1.5.1.2 | http://www.maxquant.org), which includes the Andromeda search algorithm (Jurgen Cox et al. 2011) for searching against the Uniprot database (version November 2014, taxonomy: *Drosophila melanogaster* | http://www.uniprot.org/). Follow-up data analysis was performed using the Perseus analysis framework (http://www.perseus-framework.org/).

Perseus (version 1.4.1.3) was used to analyze protein abundance dynamics in the different samples. ProteinGroups file was uploaded to Perseus. Rows containing proteins designated 'Only identified by site', 'Reverse' and 'Contaminant' were removed from the matrix. LFQ intensities were log-transformed (log2). LFQ Intensity columns of triplicates of Rpn8 and Rpn10 IPs were grouped. Rows which did not contain at least two valid values in at least one group were removed from the matrix. Next, columns were grouped similarly as just mentioned however now also the PPI triplicate was grouped.

To identify proteasome interacting proteins, Welch two-sided t-tests were performed for each α-Rpn8 or α-Rpn10 IP versus the α-PPI IPs. First groups (right) were the LFQ intensities of Rpn8 or Rpn10 IPs, second groups (left) were the LFQ intensities of PPI IPs. Permutation-based FDR of 0.05 was used for truncation. Number of randomizations was 250. –Log10 scale. Annotations were added to the tables. Tables containing the significant proteins for each two-sample t-tests were exported to excel. R was used to merge the tables for the α-Rpn8 or α-Rpn10 comparisons with α-PPI IPs based on the common 'id' columns. Rows containing significant proteins in α-Rpn8 and α-Rpn10 comparisons were merged using R and table was used to describe proteasome interacting proteins.

To identify dynamic proteasome interacting proteins, Welch two-sided t-tests were performed for each α-Rpn8 + stress or α-Rpn10+stress IP versus the Mock α-Rpn8 or α-Rpn10 IPs (thus excluding the PPI samples). First groups (right) were the LFQ intensities of either α-Rpn8+stress or α-Rpn10+stress IPs, second groups (left) were either the LFQ intensities of α-Rpn8 Mock IPs or α-Rpn10 mock IPs. Permutation-based FDR of 0.05 was used for truncation. Number of randomizations was 250. –Log10 scale. Annotations were added to the tables. Tables containing the significant proteins for each two-sample t-test were exported to excel. R was used to merge the tables for the α-Rpn8+stress or αRpn10+stress comparisons with mock IPs based on the common 'id' columns. Rows containing significant proteins in α-Rpn8 and α-Rpn10 comparisons were merged using R and table was used to describe dynamic proteasome interacting proteins.

References

Andersen, K.M. et al., 2009. Thioredoxin Txnl1/TRP32 Is a Redox-active Cofactor of the 26 S Proteasome. *Journal of Biological Chemistry*, 284(22), 15246–15254.

Arndt, V., Rogon, C. & Höhfeld, J., 2007. To be, or not to be - Molecular chaperones in protein degradation. *Cellular and Molecular Life Sciences*, 64(19–20), pp.2525–2541.

Bader, M. et al., 2011. A conserved F box regulatory complex controls proteasome activity in Drosophila. *Cell*, 145(3), pp.371–382.

Barrault, M.-B. et al., 2012. Dual functions of the Hsm3 protein in chaperoning and scaffolding

regulatory particle subunits during the proteasome assembly. *Proceedings of the National Academy of Sciences of the United States of America*, 109(17), pp.E1001-10.

van den Berg, D.L.C. et al., 2010. An Oct4-Centered Protein Interaction Network in Embryonic Stem Cells. *Cell Stem Cell*, 6(4), pp.369–381.

Bohn, S. et al., 2013. Localization of the regulatory particle subunit Sem1 in the 26S proteasome. *Biochemical and Biophysical Research Communications*, 435(2), pp.250–254.

Brand, M.D., 2010. The sites and topology of mitochondrial superoxide production. *Exp Gerontol.*, 45(7-8): 466–472.

Breusing, N. & Grune, T., 2008. Regulation of proteasome-mediated protein degradation during oxidative stress and aging Introduction: protein degradation and the proteasome. Biol. Chem, 389, pp.203–209.

Brewer, J.W. et al., 1999. Mammalian unfolded protein response inhibits cyclin D1 translation and cell-cycle progression. *Proceedings of the National Academy of Sciences of the United States of America*, 96(15), pp.8505–10.

Bull, V.H. & Thiede, B., 2012. Proteome analysis of tunicamycin-induced ER stress. *Electrophoresis*, 33(12), pp.1814–23.

Bush, K.T., Goldberg, A.L. & Nigam, S.K., 1997. Proteasome Inhibition Leads to a Heat-shock Response , Induction of Endoplasmic Reticulum Chaperones , and Thermotolerance. *The Journal of biological chemistry*, 272(14), pp.9086–9092.

Carrera, P. et al., 2003. Tousled-like kinase functions with the chromatin assembly pathway regulating nuclear divisions. *Genes and Development*, 17(20), pp.2578–2590.

Chalkley, G.E. et al., 2008. The Transcriptional Coactivator SAYP Is a Trithorax Group Signature Subunit of the PBAP Chromatin Remodeling Complex. *Molecular and Cellular Biology*, 28(9), pp.2920–2929.

Chalkley, G. E. and Verrijzer, C. P. (2004) 'Immuno-Depletion and Purification Strategies to Study Chromatin-Remodeling Factors In Vitro', *Methods in Enzymology*, 377(2001), pp. 421–442.

Chen, L. and Madura, K. (2002) 'Rad23 Promotes the Targeting of Proteolytic Substrates to the Proteasome', *molecular and cellular biology*, 22(13), pp. 4902–4913

Chen, X. et al., 2007. Ubiquitin-Independent Degradation of Cell-Cycle Inhibitors by the REG?? Proteasome. *Molecular Cell*, 26(6), pp.843–852.

Chow, C.Y., Wolfner, M.F. & Clark, A.G., 2013. Using natural variation in Drosophila to discover previously unknown endoplasmic reticulum stress genes. *Proceedings of the National Academy of Sciences of the United States of America*, 110(22), pp.9013–8.

Chu-Ping, M., Slaughter, C.A. & DeMartino, G.N., 1992. Identification, purification, and characterization of a protein activator (PA28) of the 20 S proteasome (macropain). *Journal of Biological Chemistry*, 267(15), pp.10515–10523.

Chuang, S.-M. et al., 2005. Proteasome-mediated degradation of cotranslationally damaged proteins involves translation elongation factor 1A. *Molecular and cellular biology*, 25(1), pp.403–13.

Elsasser, S. et al., 2002. Proteasome subunit Rpn1 binds ubiquitin-like protein domains. *Nature Cell Biology*, 4(9), pp.725–730.

Elsasser, S. & Finley, D., 2005. Delivery of ubiquitinated substrates to protein-unfolding machines. *nature cell biology*, 7(8). Pp. 742-749

Fabre, B. et al., 2015. Deciphering preferential interactions within supramolecular protein complexes: the proteasome case. *Molecular systems biology*, 11, p.771.

Finley, D., 2009. Recognition and Processing of Ubiquitin-Protein Conjugates by the Proteasome. *Annual review of biochemistry,* pp. 477–513

Fransen, M. et al., 2012. Role of peroxisomes in ROS/RNS-metabolism: Implications for human disease. *Biochimica et Biophysica Acta* - Molecular Basis of Disease, 1822(9), pp.1363–1373.

Fribley, A., Zeng, Q. & Wang, C., 2004. Proteasome Inhibitor PS-341 Induces Apoptosis

through Induction of Endoplasmic Reticulum Stress-Reactive Oxygen Species in Head and Neck Squamous Cell Carcinoma Cells. *Society*, 24(22), pp.9695–9704.

Funakoshi, M., 2004. Sem1, the yeast ortholog of a human BRCA2-binding protein, is a component of the proteasome regulatory particle that enhances proteasome stability. *Journal of Cell Science*, 117(26), 6447–6454.

Geetha, T. et al., 2008. p62 serves as a shuttling factor for TrkA interaction with the proteasome. *Biochemical and Biophysical Research Communications*, 374(1), pp.33–37.

Giot, L. et al., 2003. A protein interaction map of Drosophila melanogaster. *Science* (New York, N.Y.), 302(5651), pp.1727–36.

Glickman, M.H. et al., 1998. The regulatory particle of the Saccharomyces cerevisiae proteasome. *Molecular and cellular biology*, 18(6), pp.3149–3162.

Goldberg, A.L., 2003. Protein degradation and protection against misfolded or damaged proteins. *Nature*, 426, pp.895–899.

Gorbea, C. et al., 2010. A Protein Interaction Network for Ecm29 Links the 26 S Proteasome to Molecular Motors and Endosomal Components. *Journal of Biological Chemistry*, 285(41), 31616–31633

Gorbea, C. et al., 2004. Characterization of mammalian Ecm29, a 26 S proteasome-associated protein that localizes to the nucleus and membrane vesicles. *Journal of Biological Chemistry*, 279(52), pp.54849–54861.

Groll, M. et al., 1997. Structure of 20S proteasome from yeast at 2.4 A resolution. *Nature*, 386(6624), pp.463–471.

Grune, T. et al., 2011. HSP70 mediates dissociation and reassociation of the 26S proteasome during adaptation to oxidative stress. *Free Radical Biology and Medicine*, 51(7), pp.1355–1364.

Guerrero, C., 2005. An Integrated Mass Spectrometry-based Proteomic Approach: Quantitative Analysis of Tandem Affinity-purified in vivo Cross-linked Protein Complexes (qtax) to Decipher the 26 s Proteasome-interacting Network. *Molecular & Cellular Proteomics*, 5(2), pp.366–378.

Guruharsha, K.G. et al., 2011. A Protein Complex Network of Drosophila melanogaster. *CELL*, 147, pp.690–703.

Hanna, J. et al., 2007. A Ubiquitin Stress Response Induces Altered Proteasome Composition. *Cell*, 129(4), pp.747–759.

Haratake, K. et al., 2016. KIAA0368 -deficiency affects disassembly of 26S proteasome under oxidative stress condition. *Journal of Biochemistry*, 159(6), pp.609–618.

Harding, H.P., Zhang, Y. & Ron, D., 1999. Protein translation and folding are coupled by an endoplasmic-reticulum-resident kinase. *Nature*, 397(6716), pp.271–274.

Hirano, H., Kimura, Y. & Kimura, A., 2015. Biological significance of co- and post-translational modifications of the yeast 26S proteasome. *Journal of Proteomics*, 134, pp.37–46.

Hiyama, H. et al., 1999. Interaction of hHR23 with S5a. The Ubiquitin-Like Domain Of Hhr23 Mediates Interaction With S5a Subunit Of 26 S Proteasome*. *The Journal of biological chemistry*, 274(39), pp.28019–28025.

Ho Min Kim, Yadong Yu, and Y.C., 2008. Structure characterization of the 26S proteasome. *Biochim Biophys Acta*, 141(4), pp.520–529.

Holmström, K.M. & Finkel, T., 2014. Cellular mechanisms and physiological consequences of redox-dependent signalling. *Nature reviews. Molecular cell biology*, 15(6), pp.411–21.

Husnjak, K. et al., 2008. Proteasome subunit Rpn13 is a novel ubiquitin receptor. *Nature*, 453(7194), pp.481–488.

Jacobson, A.D. et al., 2014. Autoregulation of the 26S proteasome by in situ ubiquitination. Molecular biology of the cell, 25(12), pp.1824–35

Jarosch, E. et al., 2002. Protein dislocation from the ER requires polyubiquitination and the AAA-ATPase Cdc48. *Nature Cell Biology*, 4.

Jung, T. & Grune, T., 2008. The proteasome and its role in the degradation of oxidized proteins. *IUBMB Life*, 60(11), pp.743–752.

Kaake, R.M. et al., 2011. Characterization of Cell Cycle Specific Protein Interaction Networks of the Yeast 26S Proteasome Complex by the QTAX Strategy. *J Proteome Res*. 72(2), pp.181–204.

Kaneko, T. et al., 2009. Assembly Pathway of the Mammalian Proteasome Base Subcomplex Is Mediated by Multiple Specific Chaperones. *Cell*, 137(5), pp.914–925.

Kettern, N. et al., 2010. Chaperone-assisted degradation: Multiple paths to destruction. *Biological Chemistry*, 391(5), pp.481–489.

Kikukawa, Y. et al., 2005. Unique proteasome subunit Xrpn 10c is a specific receptor for the antiapoptotic ubiquitin-like protein Scythe. *FEBS Journal*, 272(24), pp.6373–6386.

Kim, D.I. & Roux, K.J., 2016. Filling the Void: Proximity-Based Labeling of Proteins in Living Cells. *Trends in Cell Biology*, 26(11), pp.804–817.

Kleijnen, M.F. et al., 2007. Stability of the proteasome can be regulated allosterically through engagement of its proteolytic active sites. Nature structural & molecular biology, 14(12), pp.1180–8.

Kupsco, A. & Schlenk, D., 2015. Oxidative Stress, Unfolded Protein Response, and Apoptosis in Developmental Toxicity. International Review of Cell and Molecular Biology, 317, pp.1–66.

De La Mota-Peynado, A. et al., 2013. The proteasome-associated protein Ecm29 inhibits proteasomal ATPase activity and in vivo protein degradation by the proteasome. *Journal of Biological Chemistry*, 288(41), pp.29467–29481.

Lam, Y.A. et al., 1997. Editing of ubiquitin conjugates by an isopeptidase in the 26S proteasome. *Nature*, 385, pp.737–740.

Lee, A.-H. et al., 2003. Proteasome inhibitors disrupt the unfolded protein response in myeloma cells. *Proceedings of the National Academy of Sciences of the United States of America*, 100(17), pp.9946–51.

Leggett, D.S. et al., 2002. Multiple Associated Proteins Regulate Proteasome Structure and Function. *Molecular Cell*, 10(3), pp. 495–507

Li, X. et al., 2006. The SRC-3/AIB1 coactivator is degraded in a ubiquitin- and ATP-independent manner by the REG?? proteasome. *Cell*, 124(2), pp.381–392.

Livak, K.J. & Schmittgen, T.D., 2001. Analysis of relative gene expression data using real-time quantitative PCR and the 2(-Delta Delta C(T)) Method. Methods (San Diego, Calif.), 25(4), pp.402–8.

Loidl, G. et al., 1999. Bifunctional inhibitors of the trypsin-like activity of eukaryotic proteasomes. *Chemistry and Biology*, 6(4), pp.197–204.

Marques, A.J. et al., 2009. Catalytic mechanism and assembly of the proteasome. *Chemical Reviews*, 109(4), pp.1509–1536.

Matiuhin, Y. et al., 2008. Extraproteasomal Rpn10 Restricts Access of the Polyubiquitin-Binding Protein Dsk2 to Proteasome. *Molecular Cell*, 32(3), pp.415–425.

Mccutchen-Maloney, S.L. et al., 2000. cDNA Cloning, Expression, and Functional Characterization of PI31, a Proline-rich Inhibitor of the Proteasome*. *Journal of Biological Chemistry*, 275(24), 18557–18565

Medicherla, B. et al., 2004. A genomic screen identifies Dsk2p and Rad23p as essential components of ER-associated degradation. *EMBO reports*, 5(7), pp.692–697.

Meister, S. et al., 2007. Extensive Immunoglobulin Production Sensitizes Myeloma Cells for Proteasome Inhibition. *Cancer Res*, 67(4), pp.1783–92.

Minami, R. et al., 2010. BAG-6 is essential for selective elimination of defective proteasomal substrates. *Journal of Cell Biology*, 190(4), pp.637–650.

MJ Gething, J. & Sambrook, 1992. Protein folding in the cell. *Nature*, 355, pp.242–244.

Mohrmann, L. et al., 2004. Differential targeting of two distinct SWI/SNF-related Drosophila

chromatin-remodeling complexes. *Molecular and cellular biology*, 24(8), pp.3077–88.

Mori, K., 2000. Tripartite Management Minireview of Unfolded Proteins in the Endoplasmic Reticulum. *Cell*, 101, pp.451–454.

Moriishi, K. et al., 2007. Critical role of {PA28gamma} in hepatitis C virus-associated steatogenesis and hepatocarcinogenesis. *Proceedings of the National Academy of Sciences of the United States of America*, 104(5), pp.1661–1666.

Moshkin, Y.M. et al., 2007. Functional Differentiation of SWI/SNF Remodelers in Transcription and Cell Cycle Control. *Molecular and Cellular Biology*, 27(2), pp.651–661.

Murata, S., Yashiroda, H. & Tanaka, K., 2009. Molecular mechanisms of proteasome assembly. *Nature reviews*. Molecular cell biology, 10(2), pp.104–115.

Nathan, J.A. et al., 2013. Why do cellular proteins linked to K63-polyubiquitin chains not associate with proteasomes? *The EMBO journal*, 32(4), pp.552–65.

Obeng, E.A. et al., 2006. Proteasome inhibitors induce a terminal unfolded protein response in multiple myeloma cells. *Blood*, 107(12), pp.4907–4916.

Oslowski, C.M. & Urano, F., 2013. Measuring ER stress and the unfolded protein response using mammalian tissue culture system. Methods in Enzymology, 490(508), pp.71–92.

Pankiv, S. et al., 2007. p62/SQSTM1 binds directly to Atg8/LC3 to facilitate degradation of ubiquitinated protein aggregates by autophagy*[S]. *Journal of Biological Chemistry*, 282(33), pp.24131–24145.

Paraskevopoulos, K. et al., 2014. Dss1 is a 26S proteasome ubiquitin receptor. *Molecular Cell*, 56(3), pp.453–461.

Parcellier, A. et al., 2003. HSP27 is a ubiquitin-binding protein involved in I-kappaBalpha proteasomal degradation. *Molecular and cellular biology*, 23(16), pp.5790–5802.

Pickart, C.M. & Cohen, R.E., 2004. Proteasomes and their kin: proteases in the machine age. *Nature reviews*. Molecular cell biology, 5(3), pp.177–187.

Pickering, A.M. & Davies, K.J.A., 2012. Differential roles of proteasome and immunoproteasome regulators Pa28αβ, Pa28γ and Pa200 in the degradation of oxidized proteins. *Archives of Biochemistry and Biophysics*, 523(2), pp.181–190.

Pilyugin, M. et al., 2009. Phosphorylation-mediated control of histone chaperone ASF1 levels by tousled-like kinases. *PLoS ONE*, 4(12), pp.1–6.

Raynes, R., Pomatto, L.C.D. & Davies, K.J.A., 2016. Degradation of oxidized proteins by the proteasome: Distinguishing between the 20S, 26S, and immunoproteasome proteolytic pathways. *Molecular Aspects of Medicine*, pp.1–15.

Rechsteiner, M. & Hill, C.P., 2005. Mobilizing the proteolytic machine: Cell biological roles of proteasome activators and inhibitors. *Trends in Cell Biology*, 15(1), pp.27–33.

Reinheckel, T. et al., 1998. Comparative resistance of the 20S and 26S proteasome to oxidative stress. *The Biochemical journal*, 335, pp.637–42.

Reinheckel, T. et al., 2000. Differential impairment of 20S and 26S proteasome activities in human hematopoietic K562 cells during oxidative stress. *Archives of biochemistry and biophysics*, 377(1), pp.65–8.

Ri, M. (2016). Endoplasmic-reticulum stress pathway-associated mechanisms of action of proteasome inhibitors in multiple myeloma. *International Journal of Hematology*, 104, 273

Richly, H. et al., 2005. A series of ubiquitin binding factors connects CDC48/p97 to substrate multiubiquitylation and proteasomal targeting. *Cell*, 120(1), pp.73–84.

Sap, K.A. et al., 2015. Global quantitative proteomics reveals novel factors in the ecdysone signaling pathway in Drosophila melanogaster. *Proteomics*, 15(4), pp.725–738.

Sap, K.A. et al., 2017. Quantitative Proteomics Reveals Extensive Changes in the Ubiquitinome

after Perturbation of the Proteasome by Targeted dsRNA-Mediated Subunit Knockdown in Drosophila. *Journal of Proteome Research*, 16(8), pp.2848–2862.

Scanlon, T.C. et al., 2009. Isolation of human proteasomes and putative proteasome-interacting proteins using a novel affinity chromatography method. *Experimental Cell Research*, 315(2), pp.176–189.

Schieber, M and Chandel, N.S., 2014. ROS Function in Redox Signaling and Oxidative Stress. Curr Biol., 24(10), 453–462.

Schmidt, M. et al., 2005. Proteasome-associated proteins: Regulation of a proteolytic machine. *Biological Chemistry*, 386(8), pp.725–737.

Seibenhener, M. & Babu, J., 2004. Sequestosome 1 / p62 Is a Polyubiquitin Chain Binding Protein Involved in Ubiquitin Proteasome Degradation. *Molecular and Cellular Biology*, 24(18), pp.8055–8068.

Sone, T. et al., 2004. Sem1p Is a Novel Subunit of the 26 S Proteasome from Saccharomyces cerevisiae, *Journal of Biological Chemistry*, 279(27), 28807–28816

Le Tallec, B. et al., 2009. Hsm3/S5b Participates in the Assembly Pathway of the 19S Regulatory Particle of the Proteasome. *Molecular Cell*, 33(3), pp.389–399.

Tomko, R.J. & Hochstrasser, M., 2014. The Intrinsically Disordered Sem1 Protein Functions as a Molecular Tether during Proteasome Lid Biogenesis. *Molecular Cell*, 53(3), pp.433–443.

Tong, L. et al., 2015. Reactive oxygen species in redox cancer therapy. *Cancer Letters*, 367, pp.18–25.

Jurgen Cox, J. et al., 2011. Andromeda: A Peptide Search Engine Integrated into the MaxQuant Environment. J. *Proteome Res*, 10, pp.1794–1805.

Varnaite, R. & MacNeill, S.A., 2016. Meet the neighbors: Mapping local protein interactomes by proximity-dependent labeling with BioID. *Proteomics*, 16(19), pp.2503–2518.

Verma, R. et al., 2004. Multiubiquitin chain receptors define a layer of substrate selectivity in the ubiquitin-proteasome system. *Cell*, 118(1), pp.99–110.

Verma, R. et al., 2000. Proteasomal proteomics: identification of nucleotide-sensitive proteasome-interacting proteins by mass spectrometric analysis of affinity-purified proteasomes. *Molecular biology of the cell*, 11(10), pp.3425–3439.

Verma, R. et al., 2002. Role of Rpn11 Metalloprotease in Deubiquitination and Degradation by the 26S Proteasome. *Science*, 298(5593), pp.611–615.

Voges, D., Zwickl, P. & Baumeister, W., 1999. The 26S proteasome: a molecular machine designed for controlled proteolysis. *Annual review of biochemistry*, 68(1), pp.1015–68.

Wakana, Y. et al., 2008. Bap31 Is an Itinerant Protein That Moves between the Peripheral Endoplasmic Reticulum (ER) and a Juxtanuclear Compartment Related to ER-associated Degradation. *Molecular biology of the cell*, 19, pp.1825–1836.

Walters, K.J. et al., 2002. Structural studies of the interaction between ubiquitin family proteins and proteasome subunit S5a. *Biochemistry,* 41(6), pp.1767–1777.

Wang, S. & Kaufman, R.J., 2012. The impact of the unfolded protein response on human disease. *Journal of Cell Biology*, 197(7), pp.857–867.

Wang, X. et al., 2007. Mass spectrometric characterization of the affinity-purified human 26S proteasome complex. *Biochemistry*, 46(11), pp.3553–3565.

Wang, X. & Huang, L., 2008. Identifying dynamic interactors of protein complexes by quantitative mass spectrometry. *Molecular & cellular proteomics. MCP*, 7(1), pp.46–57.

Wang, X.Y.J., Kaiser, P. & Huang, L., 2011. Regulation of the 26S proteasome complex during oxidative stress. *Sci Signal.*, 3(151), pp.1–17.

Yamamoto, N. et al., 2007. Proteasome inhibition induces glutathione synthesis and protects cells from oxidative stress: Relevance to Parkinson disease. *Journal of Biological Chemistry*, 282(7), pp.4364–4372.

Yao, T. et al., 2008. Distinct Modes of Regulation of the Uch37 Deubiquitinating Enzyme in the Proteasome and in the Ino80 Chromatin-Remodeling Complex. *Molecular Cell*, 31(6), pp.909–917.

Zaiss, D.M.W. et al., 2002. PI31 is a modulator of proteasome formation and antigen processing. *Proceedings of the National Academy of Sciences of the United States of America*, 99(22), pp.14344–9.

Zaiss, D.M.W. et al., 1999. The proteasome inhibitor PI31 competes with PA28 for binding to 20S proteasomes. FEBS Letters, 457(3), pp.333–338.

Zhang, N.Y. et al., 2011. Ubiquitin chain trimming recycles the substrate binding sites of the 26 S proteasome and promotes degradation of lysine 48-linked polyubiquitin conjugates. *Journal of Biological Chemistry*, 286(29), pp.25540–25546.

Zhang, Z. & Zhang, R., 2008. Proteasome activator PA28c regulates p53 by enhancing its MDM2-mediated degradation. *The EMBO Journal*, 2725, pp.852–864.

Supporting information available in this thesis

Supplementary Table S1. Proteasome co-precipitating factors

Supplementary Table S2. Dynamic proteasome co-precipitating factors

Suppl. Table1. Average LFQ intensities and significant abundant proteins in α-Rpn8 and α-Rpn10 IPs

Protein IDs	Mock_PPI	Mock_Rpn8	MG132_Rpn8	TM_24h_Rpn8	H2O2_30m_Rpn8	H2O2_24h_Rpn8	Mock_PPI	Mock_Rpn10	MG132_Rpn10	TM_24h_Rpn10	H2O2_30m_Rpn10	H2O2_24h_Rpn10	Gene names	Protein names	Description	Mock	MG132/Lact	TM	30min H2O2	24h H2O2
Q9XZJ4	28	30	32	29	29	30	28	31	33	31	31	32	Prosalpha1	Prosalpha1	Proteasome subunit	+	+	+	+	+
P40301	25	30	32	29	29	29	26	30	33	31	31	32	Pros25	Prosalpha2	Proteasome subunit	+	+	+	+	+
P18053	26	29	32	29	28	29	27	30	33	30	31	32	Pros29	Prosalpha3	Proteasome subunit	+	+	+	+	+
P22769	25	29	32	29	29	30	26	30	33	30	32	32	Pros28.1	Prosalpha4	Proteasome subunit	+	+	+	+	+
Q95083	24	29	31	28	29	28	25	30	32	30	31	31	Prosalpha5	Prosalpha5	Proteasome subunit	+	+	+	+	+
P12881	24	28	32	28	29	29	25	30	33	31	31	32	Pros35	Prosalpha6	Proteasome subunit	+	+	+	+	+
Q9V5C6	23	29	31	29	28	29	24	30	33	31	31	32	Prosalpha7	Prosalpha7	Proteasome subunit	+	+	+	+	+
A0AQH0	23	29	31	29	29	29	24	29	32	30	31	32	Prosbeta1	Prosbeta1	Proteasome subunit	+	+	+	+	+
Q9VUJ1	23	29	31	29	29	29	24	30	32	30	31	32	Prosbeta2	Prosbeta2	Proteasome subunit	+	+	+	+	+
Q9XYN7	24	28	31	28	29	29	24	29	32	30	30	31	Prosbeta3	Prosbeta3	Proteasome subunit	+	+	+	+	+
Q9VJJ0	22	29	31	28	29	29	22	29	32	30	31	32	Prosbeta4	Prosbeta4	Proteasome subunit	+	+	+	+	+
Q7K148	24	29	31	28	28	28	25	29	32	30	30	31	Prosbeta5	Prosbeta5	Proteasome subunit	+	+	+	+	+
P40304	25	29	31	28	29	29	26	30	33	30	31	31	Pros26	Prosbeta6	Proteasome subunit	+	+	+	+	+
Q9VNA5	23	28	31	28	28	28	24	29	32	30	30	31	Prosbeta7	Prosbeta7	Proteasome subunit	+	+	+	+	+
Q7KMQ0	29	33	34	34	34	34	30	34	34	35	35	35	Rpt1	Rpt1	Proteasome subunit	+	+	+	+	+
P48601	29	33	34	34	34	34	30	34	34	34	35	34	Pros26.4	Rpt2	Proteasome subunit	+	+	+	+	+
Q9V405	30	34	34	35	35	34	30	34	35	35	35	35	Rpt3	Rpt3	Proteasome subunit	+	+	+	+	+
Q9W414	29	33	34	34	34	34	29	34	34	35	35	35	Rpt4	Rpt4	Proteasome subunit	+	+	+	+	+
Q9V3V6	29	33	33	34	34	34	30	33	34	34	34	34	Tbp-1	Rpt5	Proteasome subunit	+	+	+	+	+
O18413	30	34	34	34	34	34	30	34	34	35	35	35	Pros45	Rpt6	Proteasome subunit	+	+	+	+	+
Q9VW54	31	35	35	35	36	36	31	35	35	36	36	36	Rpn1	Rpn1	Proteasome subunit	+	+	+	+	+
Q9V3P6	31	35	36	36	36	36	31	35	35	36	36	37	Rpn2	Rpn2	Proteasome subunit	+	+	+	+	+
P25161	29	34	34	35	35	35	29	34	34	35	35	35	Rpn3	Rpn3	Proteasome subunit	+	+	+	+	+
Q9V3Z4	28	34	34	35	35	35	29	34	34	35	35	35	Rpn5	Rpn5	Proteasome subunit	+	+	+	+	+
Q7KLV9	28	34	34	35	35	35	29	34	34	35	35	35	Rpn6	Rpn6	Proteasome subunit	+	+	+	+	+
Q9V3G7	29	34	34	35	35	35	29	33	34	35	35	35	Rpn7	Rpn7	Proteasome subunit	+	+	+	+	+
P26270	28	33	34	35	34	35	29	33	34	34	35	35	Mov34	Rpn8	Proteasome subunit	+	+	+	+	+
Q7KMP8	27	33	34	35	35	35	28	33	34	34	35	35	Rpn9	Rpn9	Proteasome subunit	+	+	+	+	+
P55035	27	32	33	33	33	33	28	33	33	35	35	35	Pros54	Rpn10	Proteasome subunit	+	+	+	+	+
Q9V3H2	27	33	33	35	35	34	28	33	33	35	35	34	Rpn11	Rpn11	Proteasome subunit	+	+	+	+	+
Q9V436	28	33	33	35	34	35	28	33	33	34	35	35	Rpn12	Rpn12	Proteasome subunit	+	+	+	+	+
Q7K2G1-2	28	33	34	34	34	34	28	33	34	34	34	35	Rpn13	Rpn13	Proteasome subunit	+	+	+	+	+
Q9XZ61	25	29	32	33	33	31	26	30	32	33	33	33	UCHL5	UCHL5	Proteasome subunit	+	+	+	+	+

Suppl. Table1. Average LFQ intensities and significant abundant proteins in α-Rpn8 and α-Rpn10 IPs

(continued)

Uniprot ID	Mock_PPI	Mock_Rpn8	MG132_Rpn8	TM_24h_Rpn8	H2O2_30m_Rpn8	H2O2_24h_Rpn8	Mock_PPI	Mock_Rpn10	MG132_Rpn10	TM_24h_Rpn10	H2O2_30m_Rpn10	H2O2_24h_Rpn10	Gene name	Protein name	Description	Mock	MG132/Lact	TM	30m H2O2	24h H2O2
Q9VKZ8	22	27	26	24	24	24	23	28	28	27	26	26	USP14	USP14	Proteasome subunit	+	+	+	+	+
Q9VH79	24	28	29	28	28	28	25	29	29	29	29	30	Rpt3R	Rpt3R	ATPase	+	+	+	+	+
Q9VA54	22	27	27	26	26	26	22	27	27	27	27	27	Rpt6R	Rpt6R	ATPase	+	+	+	+	+
Q9VM46	21	26	25	25	25	26	21	24	25	25	25	26	CG13779	sem1	Proteasome assembly chaperone, Proteasome 19S subunit	+	+	+	+	+
Q9V677	26	30	32	29	29	29	26	30	32	30	30	31	ECM29 homolog	ECM29 homolog, CG8858	Proteasome inhibition, coupling of proteasomes to ER	+	+	+	+	+
Q9VYG1	25	30	30	31	30	31	25	29	29	30	30	30	CG12096	CG12096	Proteasome assembly chaperone, probable proteasome inhibitor	+	+	+	+	+
Q9VPP7	22	26	26	24	25	26	23	27	28	27	28	28	CG11885	CG11885	Probable proteasome assembly chaperone	+	+	+	+	+
Q7JWR4	21	28	28	25	26	27	23	28	29	28	29	28	CG13319	CG13319	Colocalizes with proteasome	+	+	+	+	+
Q9VRP3	24	32	31	30	30	30	25	32	32	33	32	33	Txl	Thioredoxin-like	Protein disulfide oxidoreductase activity	+	+	+	+	+
Q9W4V8	23	26	26	26	26	24	24	27	26	27	27	27	ttm50	Tiny tim 50	Component of TIM23 complex, mediates translocation of transit peptide-containing proteins across mitochondrial inner membrane	+	+	+	+	+
B7Z120	21	23	23	23	23	23	23	26	27	27	27	26	tlk	Tousled-like kinase	Kinase, histone phosphorylation, cell cycle regulation	+	+	+	+	+
Q9VQ79-1	20	23	23	21	22	21	21	24	24	22	23	23	AIF	Isoform A of Putative apoptosis-inducing factor 1	Mitochondrial ATP synthesis coupled electron transport, Oxidoreductase, cell redox homeostasis, apoptotic process	+	+			
Q9VX82	21	23	23	###	###	###	23	24	26	23	23	23	Arpc3B	Actin-related protein 2/3 complex, subunit 3B	Structural constituent of the cytoskeleton	+	+			
Q9VFS8	26	30	29	31	31	31	27	30	29	31	30	31	CG9588	26S proteasome non-ATPase regulatory subunit 9/ Rpn4	Proteasome (base) assembly chaperone, Transciptional activator	+		+	+	+
Q9VZX9	23	25	24	24	25	24	23	25	25	26	25	24	CG9977	Adenosylhomocysteinase	Adenosylhomocysteinase activity	+		+	+	
P36872-2	23	26	24	22	22	23	24	26	25	25	24	26	tws	Twins	PP2A regulator activity, phosphatase, cell cycle, centrosome organization, Wnt signaling pathway	+				
Q8MKK1	24	26	25	23	24	24	25	27	26	26	26	27	CG30185; Gr59f	CG30185	Unknown	+				
Q8MRW1	23	25	24	22	23	24	23	25	25	24	24	25	CG40042	CG40042	Mitochondrial inner membrane translocase subunit Tim17/Tim22/Tim23/peroxisomal protein PMP24	+				
Q9V3W9	22	24	23	23	23	23	23	26	26	26	26	26	Rad23	DNA repair protein Rad23	DNA repair, shuttles polyubiquitinated proteins to proteasome, interacts with Rpn10, Rpn13 and Rpn1	+				
Q9VI57	21	22	20	21	22	21	22	24	22	23	23	23	Dpck	Dephospho-CoA kinase	Coenzyme A biosynthetic process, kinase activity	+				
Q9W0M4	21	24	22	22	22	23	22	24	24	23	23	23	CG13887	CG13887	Export of secreted proteins, export of transmembrane proteins, chaperone, targeting to ERAD	+				
Q9V637	22	23	24	24	24	23	22	25	26	27	27	27	CG8979	Proteasome inhibitor PI31 subunit	Inhibits the hydrolysis of protein and peptide substrates by the 20S proteasome. Enhances 26S proteasome function by promoting its assembly through the interaction with PSMD9 and PMSD5.		+	+	+	+

Suppl. Table1. Average LFQ intensities and significant abundant proteins in α-Rpn8 and α-Rpn10 IPs

(continued)

Uniprot ID	Mock_PPI	Mock_Rpn8	MG132_Rpn8	TM_24h_Rpn8	H2O2_30m_Rpn8	H2O2_24h_Rpn8	Mock_PPI	Mock_Rpn10	MG132_Rpn10	TM_24h_Rpn10	H2O2_30m_Rpn10	H2O2_24h_Rpn10	Gene name	Protein name	Description	Mock	MG132/Lact	TM	30m H2O2	24h H2O2
P16371-2	23	24	25	24	23	24	24	25	26	25	26	26	gro	Isoform A of Protein Groucho	Negative regulation of transcription from RNA pol II promoter, chromatin interacting protein		+	+		+
Q9Y114	20	###	22	21	21	21	21	23	24	23	22	22	CG8042	CG8042	Endomembrane protein, ERAD, mainenance lipid droplet homeostasis, apoptosis		+	+		
P82910	27	27	30	29	29	29	28	29	31	29	30	29	Hsp70Aa	Major heat shock 70 kDa protein Aa	Heat shock protein, stress response		+		+	+
P02516	23	24	27	22	23	23	24	22	28	21	22	22	Hsp23	Heat shock protein 23	Heat shock protein, stress response		+			
O97125	24	22	27	23	24	24	25	24	27	24	25	25	Hsp68	Heat shock protein 68	Heat shock protein, stress response		+			
Q9V3P3	24	27	30	27	27	27	25	26	31	26	26	25	REG	LD45860p	Proteasome activator PA28, mRNA splicing via spliceosome, regulation of G1/S transition of mitotic cell cycle, DNA damage response		+			
P14199	23	22	26	20	22	21	25	24	28	23	24	23	ref(2)P	Protein ref(2)P	Clearance of protein aggregates, mitochondrion organization, transcription, regulation of secretion, autophagic vacuole		+			
M9PD65	22	23	25	23	23	23	24	25	26	24	25	24	RanGap	Ran GTPase activating protein	Regulator of Ran-dependent transport between cytoplasm and nucleus. GTPase activator for the nuclear Ras-related regulatory protein Ran		+			
Q03017-2	21	22	24	23	23	23	18	20	21	18	19	19	cact	Isoform C of NF-kappa-B inhibitor cactus	Transcription factor binding, phagocytosis, negative regulation of protein import into nucleus, developmental protein, signal transduction		+			
Q9VV89	21	22	24	21	22	21	22	24	26	23	23	23	zetaCOP	Nonclathrin coat protein zeta-COP	Oxidoreductase, phagocytosis, vesicle-mediated protein transport Golgi to ER		+			
P18489-4	23	23	25	24	23	23	24	26	26	25	25	25	Syb	Isoform D of Synaptobrevin	synaptic vesicle transport, vesicle-mediated transport		+			
Q9VJZ4	22	24	25	###	23	22	24	25	26	23	24	23	CG9306	ND-B22	NADH dehydrogenase		+			
Q7KR04	23	24	25	###	24	23	24	25	26	24	24	24	RpS15Ab	40S ribosomal protein S15Ab	Structural constituent of the ribosome, translation, mitotic spindle elongation		+			
Q9VAM6	24	25	26	23	24	24	25	26	27	25	25	26	Cisd2	CDGSH iron-sulfur domain-containing protein 2 homolog	Mitochondria membrane protein, calcium transport, autophagy		+			
Q9VLM5	23	22	26	23	23	21	24	25	28	25	25	24	DAD1	Dolichyl-diphosphooligosaccharide--protein glycosyltransferase subunit DAD1	Translocation of proteins into or across the rough ER membrane.		+			
Q9VSF3	20	###	23	###	###	###	20	21	24	21	21	21	CG7375	Nedd8-conjugating enzyme Ubc12	Protein neddylation		+			
Q9VEC2	19	20	27	20	20	20	21	22	29	22	22	24	CG12321	CG12321	Assembly 20S proteasome		+			
Q9VNI4	19	20	26	###	###	###	20	20	28	20	21	22	CG2046	CG2046	Unknown		+			
Q9VS83	23	23	25	24	24	23	24	25	26	26	26	26	CG7546	CG7546	UBL-domain containing protein		+			

Suppl. Table1. Average LFQ intensities and significant abundant proteins in α-Rpn8 and α-Rpn10 IPs

(continued)

Uniprot ID	Mock_PPI	Mock_Rpn8	MG132_Rpn8	TM_24h_Rpn8	H2O2_30m_Rpn8	H2O2_24h_Rpn8	Mock_PPI	Mock_Rpn10	MG132_Rpn10	TM_24h_Rpn10	H2O2_30m_Rpn10	H2O2_24h_Rpn10	Gene name	Protein name	Description	Mock	MG132/Lact	TM	30m H2O2	24h H2O2
Q9VPR1	21	22	22	22	23	22	22	24	25	24	24	24	Tspo	Translocator protein, CG2789	Regulation of oxidative phosphorylation, positive regulation of apoptotic process, mitochondrial outer membrane protein			+	+	+
Q00637	22	21	22	23	23	23	24	25	24	26	25	25	Sod2	Superoxide dismutase [Mn], mitochondrial	Oxidation-reduction process, antioxidant activity			+		
Q9VCF4	23	23	24	23	25	23	23	24	25	25	25	23	AP-1sigma	AP-1sigma	Intracellular protein transport, vesicle-mediated transport, synaptic vesicle				+	
Q9VKM3	23	23	24	24	25	24	24	25	26	26	26	26	ATPsynG	ATP synthase, Lethal (2) 06225	ATP synthesis coupled proton transport				+	
Q9VQP9	21	22	22	###	22	22	22	24	24	23	24	22	CG9662	Putative oligosaccharyltransferase complex subunit	Translocation of proteins into or across the rough ER membrane				+	
Q7K332	22	22	22	23	23	23	23	24	24	24	25	24	CG30159	CG30159	Unknown				+	